THE PERFORMANCE OF CONCRETE JACKING PIPES DURING INSTALLATION

By

G.W.E. Milligan and P. Norris

Report No. OUEL 1986/93

University of Oxford
Department of Engineering Science
Parks Road
Oxford
OX1 3PJ

Tel. (0865) 273162 Fax. (0865) 283301

THE PERFORMANCE OF CONCRETE JACKING PIPES DURING INSTALLATION

George W.E. Milligan[1] and Paul Norris[2]

June 1993

1. Introduction

This report presents the most important technical findings of the Oxford University pipe jacking research project, in particular those arising from the site monitoring of actual construction activities. This involved the incorporation into five pipe jacks of an instrumented pipe and other instrumentation as shown in Figure 1.1. Reference should be made elsewhere (see section 10) for: details of the planning, sponsorship, funding and management of the project; instrumentation design, calibration and performance; and site selection and monitoring procedures.

The report starts by addressing the importance of pipeline alignment, the inadequacy of current specifications, and the results achievable in practice. The method of calculating three-dimensional angular misalignments between pipes from standard line and level measurements is given, and a simple site procedure for ensuring that steering corrections are made rationally is proposed.

Total pipe jacking forces depend greatly on whether the ground collapses or squeezes onto the pipe during jacking, or whether the initial overbreak around the pipe is maintained. These questions are approached via a simple understanding of the geotechnical conditions, for both cohesive and cohesionless soils, and the effectiveness of bentonite slurry support systems discussed.

Information is then provided on the measured local interface stress behaviour between the pipe and the ground and its relation to the soil parameters, in a wide variety of different ground conditions. Increases in frictional resistance during delays in jacking, and reductions due to the use of lubrication, are illustrated.

Resulting total jacking resistance is then considered, in terms of contributions due to face resistance, pipe weight and soil pressures. The way in which the total force is transmitted through the pipe barrel and the joint between pipes is analysed in detail, leading to rational approaches for pipe design under the installation loads.

Finally, the ground movements likely to occur during and after construction of a pipeline or tunnel by pipe jacking are reviewed. The areas of uncertainty still outstanding are then summarised and the further research programmes to investigate them detailed.

This report is written with the intention of benefitting all those involved in pipe jacking, whether client, consultant or contractor. Specification, design, estimating, site operation and control, resolution of claims, or preferably avoidance of the situations that lead to claims, and even the costs of insuring works, should all benefit from a better fundamental understanding of the processes involved. In the long term this should lead to more economical and safer construction and improved performance.

Most of the information in this report has been obtained from the research work on the five schemes detailed in Table 1.1. While the research work has of necessity concentrated on pipe jacked tunnels of man-entry size, the basic principles should apply equally to microtunnelling provided the consequences of the reduced diameter are taken properly into account, for example in assessing the stability of the excavated bore and hence the likely contact stresses between pipe and ground.

1. Department of Engineering Science, Oxford University and Geotechnical Consulting Group
2. Mott MacDonald, formerly Department of Engineering Science, Oxford University

	1	2	3	4	5
Date	August 1990	January 1991	March 1991	July 1991	December 1991
Location	Bolton, Lancs	Gateshead, Tyneside	Honor Oak, SE London	Chorley, Lancs	Cheltenham, Glos
Client	NW Water Bolton M.B.C	Northumbrian Water	Thames Water	NW Water Chorley D.C.	Severn Trent Water Cheltenham BC
Consultant	---	---	Binnie/Taylor Woodrow	Halcrow	---
Contractor	Laserbore	DCT	Barhale	Barhale	Lilley
Pipe Supplier	Buchan	ARC	Buchan	Spun Concrete	Spun Concrete
Pipe I.D (mm)	1200	1350	1800	1500	1200
Ground Type	Stiff Glacial Clay	Weathered Mudstone	London Clay	Dense Silty Sand	Loose Sand & Gravel
Cover (m)	1.3 - 1.5	7 - 11	11 - 21	7 - 10	4 - 7
Drive Length (m)	60	110 *	78	158	384
Position of Test Pipe	Pipe No.3	Pipe No.10	Pipe No.15	Pipe No.16	85m from front end.
Lubrication	No	No	No	No/Yes	Yes
Packer +	MDF	MDF	MDF	MDF	MDF
Excavation	Hand	Hand	Hand	Hand	Slurry T.B.M.

Notes: * Monitoring only for part of drive
+ MDF = Medium Density Fibreboard

Table 1.1 Details of schemes monitored (Norris 1992b)

2. **Pipeline alignment**

2.1 *Significance of pipeline alignment*

In the sections that follow, it will be seen that the degree of misalignment between pipes within the pipe string is of considerable significance for a number of reasons, for instance in generating additional interface friction between pipes and soil and most notably in controlling the total jacking load that can be transmitted safely through the pipe joints. By misalignment is meant the angular deviation between the central axes of successive pipes. In an ideal pipe jack, no such deviations would exist, but in practice irregularities in ground conditions, excavation methods, etc., will inevitably cause the shield at the front to stray from the ideal course; corrections are continually made with the steering jacks to maintain the line and level as close as possible to that required.

The normal practice at present is to specify limits to the allowable errors in line and level at any point along the tunnel, typically 50 or 75mm. While these may be necessary to maintain adequate clearance from obstructions or other services, or to provide correct hydraulic flow conditions, they are quite insufficient as a means of controlling the angular deviations between successive pipes within acceptable limits for transmission of large axial forces. Likewise, the allowable angular deviations specified in BS5911 relate only to the satisfactory performance of the joint sealing arrangements, not the transmission of longitudinal load.

2.2 *Alignments achieved in practice*

Figures 2.1 to 2.4 show the measured pipe joint angles ß (in three dimensions) along the pipes as constructed on four of the five instrumented sites, for various different ground conditions, cover depths, and locations within the pipe string (see Table 1.1). These joint angles were all accurately measured by the special instrumentation, but could also be determined less precisely from conventional line and level measurements, using the analysis shown in Figure 2.5. The joint angles calculated in this way are also shown. Four out of the five drives were within specified line and level throughout and typical joint angles ranged between zero and 0.3° in these reasonably well-controlled drives, with maximum values up to about 0.5°.

Successive tunnel surveys throughout the schemes showed that the alignment of the pipeline (in its unloaded state) did not change significantly as the pipeline was extended; thus local curvatures once established remain throughout the drive. This is particularly important if control during the early stages of a drive is poor, and gives rise to serious joint angles, as this is the location at which highest pipe loads will be generated later in the drive. The special instrumentation also allowed any straightening of pipe joints under load to be detected; generally any such tendency was found to be small, as shown typically in Figures 2.6 and 2.7. Only in the fully lubricated scheme 5 (Cheltenham), was any significant straightening observed, with changes in ß of about 0.08°.

2.3 *Measurement and control of pipe misalignment*

The observations reported in Section 2.2 mean that conventional line and level measurements at the shield are sufficient for practical purposes to determine joint angles, assuming that no significant change in alignment occurs due to the application of jacking loads or the passage of successive pipes. Where it is required for any reason to determine joint angles more precisely, for instance to check maximum angles where damage to pipes has occurred, this could be done using a Demec gauge to measure the distances between

points on adjacent pipes at three locations around a joint. The joint angle ß is then calculated from changes in these distances using the analysis presented in Figure 2.8.

Normal measurements of line and level may also be used in a simple method of making sensible decisions on steering adjustments to keep angular deviations within acceptable limits. Consider the lead pipe in the tunnel, for which the current line and level errors are measured to be X_1, Y_1, plotted as point A on the "control diagram", Figure 2.9. The tunnel is now advanced by one pipe length, usually 2.5m, after which the line and level errors are X_2, Y_2, point B on the diagram. If the tunnel is then to be advanced a further pipe length, pipe N°2 will end up in the position previously occupied by pipe N°1, with the offsets of its two ends given by points A and B. If pipe N°1 were to continue along exactly the same alignment, with no angular deviation at the joint with pipe N° 2, the new line and level errors at its front end would be given by point C with co-ordinates X_3, Y_3 such that $(X_3-X_2) = (X_2-X_1)$ and $(Y_3-Y_2) = (Y_2-Y_1)$, as shown on the figure. However if there is an angular deviation of the joint of ß = 0.1°, the end point of pipe N° 1 could lie anywhere on the circle with radius R_1; for ß = 0.2° the corresponding circle would have radius R_2, and for ß = 0.5° radius R_3. In each case the radius of the circle would be given by $R = L$ß where ß is in radians and L is the pipe length. Converting ß to degrees and putting L as 2500mm, gives R = 43.6ß (mm).

The controlling engineer, lead miner or computer may then make a rational decision as to how line and level should be corrected over this next pipe length. The aim would be to head towards zero error (X = 0, Y =0) but without exceeding an acceptable angular deviation of, say, 0.1°. The line and level at the end of this stage, point D, should then be within an area as shown hatched in the figure. This would require the front end of the pipe to go from B to D, the necessary adjustments to the steering jacks being indicated by the change in direction from line BC to line BD. In the example shown this would indicate an adjustment to the vertical alignment but very little to the horizontal alignment. For the next pipe length, the process is repeated starting from what are now the last two data points, B and D. On site it would probably be most practical to have the control diagram on a plastic sheet so that points could be marked with a felt tip pen and easily removed once no longer needed, with the circles drawn to the correct scale on a transparent overlay sheet.

The method easily allows flexibility of decision-making; for instance corrections can be deliberately biased towards controlling level at the expense of line should the former be of greater consequence. It would also be possible to plan "moves" ahead if it is necessary to get an off-line drive back accurately on line by a particular chainage, for instance at an existing shaft, while ensuring that angular misalignments are acceptable. However the greatest benefit on site might be psychological, in emphasising to all concerned the importance of keeping angular deviations small, and providing a simple graphical method of observing the actual deviations occurring as the tunnel progresses.

Note that in all the above discussion of joint angles, these may easily be converted into differential joint gaps, or vice versa. A joint angle ß is related to a maximum differential joint gap δ at the internal surface of the pipe by the relation

$$\delta = \pi ß D/180$$

where ß is expressed in degrees and D is the internal diameter of the pipe.

3. **Tunnel stability and ground closure**

3.1 *Tunnel stability*

The stability of the excavated bore is of considerable importance in pipe jacking, for a number of reasons: sudden collapses may endanger miners or damage tunnelling machinery; large ground movements above the pipeline may be caused, damaging foundations, road pavements or other service runs; and ground collapsed onto the pipeline will greatly increase the resistance to jacking and probably lead to excessive total jacking forces. The first two of these generally relate to the excavated face at the front of the shield. Ground conditions should be carefully assessed to anticipate possible face instabilities, particularly in mixed ground, soft clays and silts, or cohesionless soils below the water table. Where any possibility of collapse exists, consideration should be given to the use of earth-pressure balance or slurry support tunnelling machines. Face stability in cohesive soils may be assessed from the analysis given in Figure 3.1. Note that if the shield is kept tight against or embedded into the face the ratio P/D is zero. When the undrained strength is reasonably high, no face pressure is needed. When face pressure is needed, it must be kept within limits to ensure that neither excessive settlement nor heave occurs. A factor of safety of 2.0 on collapse will usually ensure this, but in soft clays at shallow depth the safe range of pressures is very limited as shown in the example in the figure.

Along the pipeline behind the shield, the ideal situation is that the overbreak, due to the shield being of slightly larger external diameter than the pipes, should remain open so that the pipes are sliding along the base of an open bore. The total jacking forces will then be minimised. Stability in cohesive soils is assessed as shown in Figure 3.2, and is controlled in the short term by the undrained strength of the soil. Stability in cohesionless soils is assessed as shown in Figure 3.3, and depends on the angle of friction of the soil. Note that in the latter case some internal pressure in the bore is necessary to maintain stability. For fine sands above the water table this may be supplied by capillary suctions, as was the case in scheme 4 of the research. Alternatively it may be provided by fluid pressure from a bentonite slurry filling the overbreak at a sufficient pressure to maintain stability. This was the approach successfully adopted in scheme 5.

3.2 *Bentonite slurry support and lubrication*

Lubrication of any kind can only work effectively if a discrete layer of the lubricant is maintained between the two sliding surfaces, in this case the exterior of the pipe and the adjacent excavated soil surface. Once the gound has collapsed onto the pipe, the effect of lubrication will be greatly reduced. The first and most important function of bentonite slurry or other lubricant is therefore to provide sufficient internal pressure to stabilise the tunnel bore as discussed above. The slurry must be designed to form a filter cake in the surrounding soil without excessive bleeding of material and be pressurised to the necessary level to overcome ground water pressures and stabilise the tunnel. Clearly it must fill the complete overbreak space before this can be achieved. In this situation, large diameter concrete pipes are theoretically buoyant. Successful lubrication of scheme 5 was achieved with slurry pressures of around 50 kPa, against a theoretical support pressure of about 10 kPa. Buoyancy of the pipes was also observed as changes in the surveyed pipe level following injection of lubricant (see Figure 2.4); that the pipe was able to lift by some 20mm indicates that the full overbreak of 20mm on diameter had been maintained. Confirmation of this was obtained from the contact stress cells, which registered total stresses equal to the slurry pressure, very low or

zero effective contact stresses with the soil at the bottom of the pipe, slightly higher effective contact stresses at the top of the pipe, and very low shear stresses.

In contrast, lubrication was also used for part of scheme 4 through mixed fine sand, silt and clay soils above the water table. In general, capillary suctions were sufficient to keep the bore stable along most of the drive, but the lubricant did not always fill the overbreak void and its effectiveness varied greatly. In some places the measured interface friction was greatly reduced, but elsewhere did not differ from the values obtained over the unlubricated length (Figures 3.4 and 3.5).

In clays of low permeability, plain water should theoretically be able to stabilise the tunnel bore and provide buoyancy to the pipe to minimise contact stresses and reduce jacking forces. However there is a danger that water, or even aquaeous slurries, may soften the clay and reduce the local ground stability and induce swelling in the soil so that the overbreak closes and contact stresses between pipe and ground are increased. Some evidence of this was obtained in scheme 1, where the ground was affected by water from a burst water main and heavy rain, and significant increases in jacking resistance were subsequently measured. However the precise reason for this increase is not known; it may be connected with a chnage in mode of sliding from frictional to cohesive, as discussed in Section 4.2. Polymer lubricants which do not give up water to the soil may still be very effective in these situations.

3.3 *Ground closure*

Even when the excavated tunnel is stable, the ground may close onto the pipe due to the "elastic" unloading of the ground around the tunnel. The reductions in vertical and horizontal diameter of the opening may be estimated from an elastic analysis as given in Figure 3.6. If these reductions exceed the initial overbreak, contact between soil and pipe will occur, radial stresses will develop, and resistance to jacking start to increase. Of the five schemes monitored, the calculated reduction in diameter was less than the initial overbreak in all except scheme 3. Here the calculated reduction in horizontal diameter is about 30mm, sufficient to close the overbreak; large contact stresses were developed in this case, in fact sufficient to damage the instrumentation.

In very stiff, heavily overconsolidated clay a further mechanism of ground closure may have to be considered. Localised stresses around the tunnel opening may be large enough to cause local plastic yielding of the soil: the resulting ground strains cannot be predicted without complex analyses (e.g. by finite elements) but as the minimum stresses to cause local yielding are exceeded the deformations will increase rapidly above those predicted from the purely elastic analysis.

4. **Pipe/soil interface behaviour**

4.1 *Local interface stresses*

The contact stress cells incorporated into the instrumentation allowed direct measurement of both radial (normal) and shear stresses at the interface between pipe and ground. Pore pressures were also measured at the interface close to the contact stress cells. Subtraction of the pore pressure from the total radial stress should give the effective radial stress, but in practice the results were often difficult to interpret for various reasons.

Figure 4.1 clearly indicates the pipes sliding along the base of a stable bore, with contact only at the bottom; stresses varied widely about mean values, probably mainly due to irregularities in the excavated surface. Similar effects were observed in scheme 2, but in scheme 3 in heavily overconsolidated London clay very large radial stresses and pore pressures were measured, particularly on the sides of the pipe. Local stresses of more than 500 kPa were sufficient to damage the instrumentation.

Results for scheme 4 are shown in Figure 4.2; again contact is mainly along the base of the tunnel, while intermittent and lower stresses on the sides and top indicate occasional contact occurring at these locations. As already mentioned in Section 3.2, in scheme 5 the instruments generally recorded the fluid pressures from the lubricating fluid and very low shear stresses. Some contact occurred between pipes and soil at the locations in the drive of maximum curvature.

4.2 *Pipe-soil friction*

Results relating local shear and radial stresses from all pushes during jacking have been plotted for each drive of schemes 1 to 3 (before instrument failure) in Figures 4.3 to 4.5. The results for scheme 4 have already been given in Figures 3.4 and 3.5. The relation between shear and total normal stresses appears to be frictional in all the ground materials, in that shear stresses increase more or less linearly with normal stresses. However in the cohesive soils, at higher stresses the shear stresses seem to tend toward a limiting value, which is probably controlled by the undrained strength of the soil multiplied by an adhesion factor such as is applied in the design of piles.

Scheme No.	Soil type	Friction angle (°)
1	Glacial clay	19
2	Mudstone	17
3	London clay	12.7
4	Silty sand	38
4	Sandy silt	30

Table 4.1 Measured local interface friction angles

For the frictional behaviour, the apparent interface friction angles are as given in Table 4.1. Values are given in terms of total stress. Values in terms of effective stress were similar but with greater scatter of data; lack of full saturation at the interface and the difference in location of the contact stress and pore pressure measurements introduced some uncertainty into the determination of effective stress and the total stress values are considered at present

to be more reliable. The values obtained are reasonable in comparison with the known typical values for these soil types.

4.3 *Effects of misalignment*

Misalignments in the pipeline must inevitably induce contact stresses between pipe and ground, for instance as shown in Figure 4.6. Site data showed that scenario (b) of this figure was a good model in many cases, with typical radii of pipeline curvature as given in the figure. The coincidence of sharp curvature and high local interface stresses is clearly shown by the results for schemes 4 and 5 in Figure 4.7. the pipeline appears in scheme 4 to act as a prestressed beam spanning between the high points, while in scheme 5 the deviations are mainly horizontal and the only large stresses are at the sides.

4.4 *Time factors*

In cohesive soils it is well known that the force needed to restart a jack after a stoppage is usually higher than that needed to maintain subsequent motion. A typical set of data from scheme 3 is shown in Figure 4.8; similar results but with much smaller increases were observed in the low plasticity clay of scheme 1. The mechanism is probably that pore pressures generated during pushing dissipate during a stoppage, so that the effective stress increases even though the total stress decreases; similar effects have been observed in high-speed interface ring-shear laboratory tests on London clay. Relations between increase in jacking load and the natural logarithm of stoppage time are shown in Figure 4.9; in scheme 3 significant increases occurred for stoppages of only a few minutes, and of around 25% in the first hour.

4.5 *Lubrication*

As already noted above, effective lubrication in which a complete annulus of lubricant was maintained between pipe and stable ground reduced the interface shear stresses in scheme 5 to very low values of around 2kPa. This is higher than the shear stress of the pure bentonite slurry (about 0.05 kPa), but is consistent with the shear strength of a slurry contaminated with sand. In scheme 4 the annulus was not completely filled, although a layer of soil-lubricant mixture typically 10mm thick was seen to have formed adjacent to the pipe over its bottom half, and the effectiveness of the lubrication was rather variable.

5. **Total jacking forces**

5.1 *Forces due to face loads*

The records of the total jacking forces, measured by load cells on the main jacks, are shown for each of the five monitored schemes in Figures 5.1 to 5.5. The intercept of the line of average increase in jacking force on the zero axis gives an indication of the face resistance. This was relatively small in the cohesive soils of schemes 1 and 3, but large in the mudstone of scheme 2. In scheme 4 the face resistance was very closely related to the excavation and trimming process at the shield. Generally the miner excavated to a diameter slightly larger than the outside diameter of the shield, and face resistance was very small. However occasionally the shield was used to trim the final 10 to 20 mm of excavation, and the face resistance then increased markedly by almost 1000 kN (100 T). In the machine-driven scheme 5 the large face resistance of about 1200 kN included the slurry face pressure and the resistance of the shield trimming the excavation. The measured face loads are summarised in Table 5.1.

		Measured face load	Average friction force	Average friction stress	Craig (1983)
Scheme		kN	(kN/m)	(kPa)	(kPa)
1	Dry Wet	120	7.2 29.8	1.5 6.2	5 - 18
2	First 40m	950	18.0	1.5	2 - 3
3		300	54.4	7.6	5 - 20
4	Unlub. Lub.	100 - 800	23.1 9.4	4.2 1.7	5 - 20
5	Unlub. Lub.	1200	100 10	22 2.2	10 - 15

Table 5.1 Average face resistance and pipeline friction

5.2 *Average friction forces*

Average friction forces for the five schemes are also included in Table 5.1. In the final two columns the resistance is expressed as an average interface shear stress and compared with the values from past experience quoted by Craig (1983). The measured values are generally at or below the Craig values, either because of the stable ground conditions or the good directional control of the jacks or a combination of the two. It is of course somewhat misleading in most cases to express the resistance as a mean shear stress, since only the bottom of the pipeline is really in contact with the soil. Points to note from the figures are: the marked increase in resistance in scheme 1 after heavy rainfall; the very low resistance for sliding on the mudstone in scheme 2 in comparison with the length over boulder clay; the very "peaky" trace in scheme 3 due to the time effects discussed above; and the marked change from unlubricated to fully lubricated behaviour in scheme 5. The rapidly increasing

resistance in scheme 5 after about 110m is probably associated with the problems of misalignment at 110 and 130m.

5.3 *Forces due to self weight of pipes*

When the pipeline is sliding along the base of a stable bore it is reasonable to assume that the average resistance should be related simply to the weight of the pipe. Using the measured local interface friction coefficients, results for the three schemes for which this model is appropriate are given in Table 5.2. Agreement between theory and measurement is quite good, though the measured values are somewhat higher, probably as a result of increased contact stresses due to misalignments. However it would seem that this approach could be useful in suitably favourable conditions; increasing the calculated resistance by about 25% to cover increases due to misalignment should give a reasonable estimate of jacking resistance.

Scheme	Field skin friction δ (°)	W tan δ (kN/m)	Av. friction (kN/m)
1	19	6.1	7.2 (dry) 29.8 (wet)
2	17	7.0	8.0
4	38 (unlub.) 15 (lub.)	18.7 6.5	23.1 9.4

Table 5.2 Pipe self weight friction

In softer clays a more appropriate model may be that of Haslem (1986), shown in Figure 5.6, in which the undrained adhesion between pipe and soil is multiplied by a contact width determined from elasticity theory. The only monitored site on which this situation occurred was in the later stages of scheme 1, after heavy rain had softened the soil. The calculation in Figure 5.6 compares very closely with the measured resistance; however more data from softer clay is needed to validate this model.

5.4 *Forces due to ground pressures*

When the ground closes onto the pipeline, the resistances will increase considerably above those considered in Section 5.3. On the monitored sites this occurred in scheme 3 and at the start of scheme 5. The evidence obtained from scheme 3 was insufficient, due to the early failure of the instruments under the very high ground pressures, to allow theoretical calculations of these pressures in heavily overconsolidated clays to be advanced.

For scheme 5, it is possible to compare the frictional resistance over the unlubricated early part of the drive with that calculated from the ground stresses shown in Figure 5.7 and following an analysis originally derived by Terzaghi (1943). The ground movements assumed in this analysis are well supported by measurements as discussed in Section 8.2. The calculation gives a total jacking resistance of 110 kN/m, compared with a measured value over the first 20m of about 100 kN/m. This shows very satisfactory agreement for drives through loose to medium-dense cohesionless materials.

5.5 *Fully lubricated drives*

As discussed above, a fully lubricated drive is one in which an annulus of lubricant is maintained between the pipe and the soil surface of a stable tunnel bore. Such conditions were achieved for much of the length of scheme 5, and the resulting jacking resistance was only about 1000 kN over a length of 100m, an average of 10 kN/m, which is equivalent to a mean interface shear stress of only 2.2 kPa, not much in excess of the shear strength of the bentonite slurry lubricant. Clearly, effective lubrication should allow long pipeline lengths to be jacked, provided good directional control is also maintained.

6. **Pipe barrel stresses**

6.1 *Load paths through pipes*

As the pipe string "wriggles" through the ground, the location of the point of maximum compression in any pipe joint will change. Such points are defined here by an angle α from the top of the pipe. Plots showing typical variations in α along a drive for the instrumented pipe joints are shown in Figures 6.1 and 6.2. The difference in α between the two ends of the pipe indicate the load path through the pipe; zero difference means that loading is essentially along one edge of the pipe, a difference of 180° that loading is diagonally across it. Either of these conditions is possible, resulting from misalignments of the types shown in Figure 4.6; as is any intermediate value, due to three-dimensionsal misalignments from simultaneous variations in line and level.

The site measurements also show that load paths may be anything from edge loading to diagonal. However, careful study of the data has shown that the diagonal case only occurs when the load is relatively small, such as close behind the shield where quite rapid changes in α occur as a result of steering operations, or at very small joint misalignment angles as the pipeline passes through a point of contraflexure in the tunnel. Neither of these situations is normally very critical for the design of the pipes; an exception would be the case immediately behind the shield in a drive with a very high face resistance. The most critical situations usually result from edge loading with high jacking forces and relatively large joint misalignment angles (ß), due to over-rapid corrections of tunnel alignment.

6.2 *Pipe barrel stresses*

Direct measurements were made of mean pipe barrel strains in the longitudinal direction using extensometers bolted to the inner surface of the instrumented pipe. A typical set of plots is shown in Figure 6.3. These may immediately be seen to correlate with the load path information in Figure 6.1; loading is initially mainly along the bottom of the pipe for the first 10m of the drive, transferring rapidly to the top at about 15m, then to the right hand side for the remainder of the drive. These observations may in turn be related to the tunnel alignment plot in Figure 2.2.

6.3 *Elastic analysis and design*

Longitudinal stresses were then determined from these strains, and compared with stresses calculated from the measured forces on the pipe, on the basis of simple stocky-column elastic theory. Agreement was generally very good. Maximum stresses in compression were within the normally recognised elastic range for the concrete, while tensile stresses on the unloaded side of the pipe were less than the tensile strength and hence would not lead to tensile cracking. This was true even for the most extremely loaded pipes, under conditions which were inducing local pipe failures at joints. It therefore appears that pipe barrels may be safely designed using simple compression theory, and that joint failure is likely to occur before the pipe barrel shows any sign of distress, at least within the range of conditions covered by the research. Only nominal longitudinal reinforcement is required, if any. Hoop reinforcement will generally be needed in larger diameter pipes to resist bending due to ground pressures, and possibly complex three-dimensional stress conditions near the pipe ends due to the jacking loads, but no information on this has been obtained from the research.

7. **Pipe joint stresses**

7.1 *Joint stress distributions*

The thin pressure cells incorporated into the joints at either end of the instrumented pipe allowed measurements to be made of the distribution of stress around the joints and its correlation with the joint misalignment angle. Typical results from four sites are shown in Figures 7.1 to 7.3. The pressures measured in individual cells are clearly related to the magnitude and orientation of the joint misalignment, and also depend on the total force transmitted. However, even at quite small misalignment angles the stresses in the joint are highly localised, perhaps acting over less than a quarter of the pipe circumference and reaching high local values at the point of maximum compression of the joint.

Precise back analysis of the results is complicated by the stress-strain behaviour of the packing material, in this case medium density fibreboard, which had been found in the laboratory testing to be the best of the common wood-based materials (see Figure 7.4). The material is initially quite compressible, but on unloading acquires a permanent compression and is then much stiffer on subsequent reloading. As the material is compressed and recompressed under different stresses at different points around the joint as it progresses through the tunnel, its behaviour at any time will reflect its stress history up to that time. However eventually it will tend everywhere towards the "previously compressed" material behaviour.

The measured joint stresses may be compared with those calculated by linear-stress theories such as that of the Australian Concrete Pipe Association (see Figure 7.5). Four such comparisons are presented in Figures 7.6 and 7.7, using appropriate linear approximations to the packer stiffness as shown in the inset figures. Agreement is generally good, with the theoretical calculation giving somewhat higher edge stresses than measured in some cases. This approach would therefore appear to provide a reasonably conservative design method.

7.2 *Joint design*

Joint design based on the above approach requires information only on a maximum allowable concrete stress, the stiffness of the packing material, and its location within the joint, to provide the maximum allowable jacking force for any specified maximum joint misalignment angle. Note that any specified joint angle should include any lack of squareness of pipes; BS5911 allows maximum angles due to lack of squareness of around 0.15°, and two pipes with opposing errors could give an angle of 0.3° in a perfectly straight pipeline. However a check on pipes manufactured in the UK showed that actual lack of squareness was typically around 0.05°, and there was no indication from the research that this was a significant factor in joint design when using pipes of this quality (see Table 7.1).

When the jacking force is well distributed over the pipe end area, it would be appropriate to use a concrete strength as in normal structural design of 0.4 times f_{cu}, the characteristic cube strength of the concrete. However, for the highly localised stresses at the joints in the extreme design conditions, a joint face stress of $0.8f_{cu}$ appears more appropriate. If a joint face strength test is performed, and the minimum stress of $70N/mm^2$ achieved, then it should be satisfactory to use this higher value.

The packer stiffness should for safety be taken as the unload-reload stiffness of the material measured over the appropriate stress range; its thickness should likewise be that of the material after precompression to the maximum expected joint stress. It should be as wide as possible, while keeping it some 20mm back from the edge of the concrete to reduce the

risk of local spalling.

Figures 7.8 to 7.10 show design charts produced on this basis, for various combinations of pipe diameter, packer width and stiffness, and allowable concrete strength. The very rapid reduction in allowable joint load with misalignment angle is apparent; typical maximum joint angles of say 0.5° will limit the jacking force for even the best combination of the above to about 400T. Figure 7.11 indicates the improved jacking forces that might be obtained with a packing material of lower stiffness and greater recovery. However it is important that any such material should also have the low Poisson's ratio of the wood-based materials, otherwise large bursting stresses will be set up in the joint.

Supplier	Spigot (β_{es})° A	Spigot (β_{es})° B	Socket (β_{em})° A	Socket (β_{em})° B	Maximum angle from BS5911 Part 120:1989	Pipe diameter (mm)
ARC	0.02	0.00	0.07	0.00	0.15	1200
	0.03	0.08	0.03	0.03	"	1200
(Spun process)	0.03	0.08	0.08	0.08	"	1200
	0.05	0.03	0.05	0.03	"	1200
Method of	0.02	0.02	0.02	0.02	"	1200
measurement CEN	0.08	0.03	0.03	0.03	"	1200
	0.05	0.09	0.00	0.09	0.14	1350
	0.02	0.05	0.02	0.05	"	1350
	0.00	0.02	0.00	0.02	"	1350
	0.03	0.02	0.07	0.02	"	1350
	0.04	0.05	0.04	0.05	"	1350
	0.00	0.02	0.00	0.02	"	1350
Spun Concrete	0.02	0.02	0.02	0.05	0.15	1200
	0.07	0.05	0.04	-	"	1200
(Spun process)	0.03	0.03	0.03	0.03	"	1200
Method of	0.07	0.07	0.07	0.06	0.13	1470
measurement CEN	0.08	0.04	0.03	0.00	"	1470
	0.07	0.04	0.07	0.04	"	1470
	0.05	0.01	0.05	0.05	0.15	1800
	0.04	0.02	-	0.02	"	1800
	0.01	0.01	0.05	0.01	"	1800
CV Buchan	0.08		-		0.15	1800
	0.09		-		"	1800
(Vertically cast)	0.09		-		"	1800
	0.06		-		"	1800
Method of measurement plumb line on roller line	0.09		-		0.14	1820
	0.08		-		0.14	1820

Notes 1. A & B refer to two planes at 90° to each other
2. - No reading taken

Table 7.1 Pipe end squareness audit (Norris 1992b)

8. **Ground movements**

8.1 *Short-term settlement and heave*

During pipe jacking, ground movements may occur due to instability of the face or the tunnel bore, or from the elastic unloading of the ground caused by the excavation. These have been discussed above in Section 3. In the research programme, detailed measurements of ground movements were only made in scheme 5. Here an array of inclinometers and magnetic settlement plates were installed at one cross section of the tunnel and vertical and horizontal movements measured. In the short term, as the tunnelling machine approached the array, movements were observed upward and ahead of the machine as shown in Figure 8.1. Surprisingly, no longitudinal movements were picked up by the inclinometer A on the centreline of the tunnel, while those recorded by inclinometer B are hard to understand. The upward movements were barely measurable at the surface, indicating that some compression occurred in the loose soils above the tunnel. These movements were probably the result of the high face load applied by the shield and face slurry pressure. The total face resistance of about 1200kN (see Figure 5.5) is equivalent to a pressure of 730 kPa over the face area, which is considerably greater than the theoretical passive earth pressure at that depth.

8.2 *Long-term settlements*

Long-term settlements will occur due to the closing of the overbreak, unless it is completely grouted as soon as construction of the pipeline is complete. Ground movements may then be assessed using the methods developed from other forms of tunnelling, with the advantage that the maximum "ground loss" is limited to the volume of the overbreak. The best estimates at present are made from empirical observations of settlements, as shown in Figure 8.2. The shape of the settlement trough has been found to approximate to an error function, and field observations allow an estimate to be made of the parameter (i), which controls the width of the trough, for cohesive and cohesionless soils. Equating the volume of the trough to the volume of the overbreak assumes of course that no volume change occurs in the soil. Dense cohesionless soils will tend to expand, reducing the settlements, while loose soils may compact and give increased settlements.

In scheme 5, the measured long-term settlements showed the expected form, except that the whole array appeared to experience an additional settlement of about 4mm, the full lateral extent of which could not be determined (see Figure 8.3). This was attributed speculatively to general compaction of the fairly loose gravelly sand due to vibrations from the tunnelling machine. Subtracting this, the surface settlements at three tunnel cross-sections were only 3 to 9mm, as shown in Figure 8.4. However it should be noted that settlements were not complete at the time of the last measurement, the trends with time for the centre-line settlements being as shown in Figure 8.5. In addition, the surface settlements were clearly influenced by the stiff road pavement. The movements measured immediately below the pavement were rather greater (Figures 8.3 and 8.5) and the centreline settlement (after subtraction of 4mm) was about 11mm at the end of the measurement period and approaching the calculated value of 12.8mm in the long term.

9. **Further Research**

While much has been learnt from the work to date, a number of aspects require further investigation. Briefly, these may be listed as:-

- radial pressure distributions on pipes, and the relation of these to soil conditions, overbreak size etc.;
- shear to normal (radial) stress relations for a wider variety of soils, in particular soft clay, and tunnel depths (stress levels);
- ground movements for various combinations of soil type and tunnel depth, overbreak volume etc.;
- stress concentrations on pipe ends at the thrust ring and adjacent to interjack stations, at which loading conditions may be severe, although the additional system flexibility associated with the interjack or main jacking set-up may allow some self-righting of eccentric loading;
- improvements to pipe joint details and packer material properties so as to allow larger jacking loads to be transmitted through misaligned joints.

The first four of these require a continuation of the site-based work, with some parallel laboratory testing to investigate interface friction behaviour. This will constitute stage 3 of the research, lasting three years from November 1992. Stage 4 will take place almost in parallel for three years from early 1993, and will concentrate mainly on the final aspect listed above; it will involve computer modelling of existing and possible alternative joint details, followed by physical modelling in the laboratory and perhaps on site of those showing most promise. The research assistant on stage 4 will also assist with site work on stage 3 as necessary. Some contributions to the work, such as to the laboratory testing for stage 3, will be made by 4th-year undergaduate projects, and there is a good possibility of acquiring a fully-supported research student (SERC or overseas) to work on some aspect of the problem, for instance the determination of short and long-term ground movements.

Stage 3 will be supported financially by SERC, the Pipe Jacking Association and a consortium of major water service companies. Stage 4 will be fully supported by SERC. Progress of the work will be monitored by a management group with representatives from the funding bodies, as was found to be very successful in stage 2; involvement of the PJA was very important in obtaining the co-operation of contractors and pipe suppliers, while the water companies provided the necessary sites on which to work and carried the additional site costs on each contract.

10. **Main conclusions**

The main conclusions from the work may be summarised as follows:-

(i) The contact stresses between pipe and ground depend on the stability of the tunnel bore, the initial stresses in the ground and the stiffness of the soil. In cohesionless materials they are well predicted by the Terzaghi model.

(ii) Pipe-soil interface sliding behaviour is frictional in nature even in cohesive soils, except that the undrained strength provides an upper bound in cohesive soils. The field behaviour is consistent with that measured in laboratory interface tests (modified shearbox).

(iii) In stable tunnel bores, the resistance to sliding of the pipes is related simply to the self weight of the pipes.

(iv) Effective lubrication requires complete filling of the overbreak, and in cohesionless soils sufficient pressure to maintain the stability of the tunnel bore. Bentonite slurries are suitable in silty, sandy and gravelly soils, but in stiff clays aquaeous slurries may accelerate swelling of the clay leading to increased contact stresses between pipe and ground.

(v) Face loads are likely to be relatively high with slurry or earth-pressure-balance tunnelling machines, but care is needed to ensure that the face is not overloaded, leading to excessive ground movements. High face loads will occur in hand drives in strong soils when the shield is used to trim the excavation.

(vi) Design of pipe barrels for jacking loads may be safely based on simple stocky-column elastic theory.

(vii) Local pipe joint stresses may be very high, but may be calculated in relation to maximum joint angles with adequate accuracy using the Australian CPA linear-stress approach. Local stresses up to 0.8 times the characteristic concrete cube strength may be allowed; alternatively the allowable stress may be based on the joint face strength test.

(viii) Within reason, joint packing materials should be as thick as possible, and as wide as possible without encroaching within 20mm of the face of the concrete. Of the common wood-based materials, medium density fibreboard or chipboard are the best. Packers should be considered as part of the pipe and fitted at the pipe works.

(ix) It is possible for pipe manufacturers to provide curves showing allowable jacking loads related to joint angles for the particular concrete strength and packing material. It would be reasonable for specifying Engineers to require contractors to remain within these allowable loads by a suitable combination of interjacks and good site control of alignment. Conventional line and level specifications should then only be related to hydraulic or other requirements. Pipe end squareness should be included when defining allowable joint angles. This approach would benefit manufacturers of high-quality pipes and contractors able to exercise good control on site.

(x) Site supervision by both clients' and contractors' staff should emphasise the control of joint angles, which may be calculated from conventional line and level measurements. A simple graphical method has been proposed which allows rational decisions about steering corrections to be made to minimise subsequent joint angles.

11. **References**

References from stage 2 of the research work

Norris, P. and Milligan, G.W.E. (1991) *Field instrumentation for monitoring the performance of jacked concrete pipes.* FMGM 91, Proc. 3rd. Int. Symp. on Field Measurements in Geomechanics, Oslo.

Milligan, G.W.E. and Norris, P. (1991) *Concrete jacking pipes, the Oxford research project.* Proc. 1st. Int. Conf. on Pipe Jacking and Microtunnelling, Pipe Jacking Association, London.

Norris, P. (1992a) *Instrument design, manufacture and calibration for use in monitoring the field performance of jacked concrete pipes.* Report No. OUEL 1919/92, Department of Engineering Science, Oxford University.

Norris, P. and Milligan, G.W.E. (1992a) *Pipe end load transfer mechanisms during pipe jacking.* Proc. Int. Conf. on Trenchless Construction, No Dig 92, Washington.

Norris, P. and Milligan, G.W.E. (1992b) *Frictional resistance of jacked concrete pipes at full scale.* Proc. Int. Conf. on Trenchless Construction, No Dig 92, Paris.

Norris, P. (1992b) *The behaviour of jacked concrete pipes during site installation.* D.Phil. thesis, University of Oxford.

Other references

Atkinson, J.H. and Mair, R.J. (1981) *Soil mechanics aspects of soft ground tunnelling.* Ground Engineering, Vol.14, No.5.

Craig, R.N. (1983) *Pipe Jacking: a State-of-the-art Review. Technical Note No. 112.* CIRIA, London.

O'Reilly, M.P. and New, B.M. (1982) *Settlements above tunnels in the United Kingdom - their magnitude and prediction.* Proceedings Tunnelling '82 Symposium, Institution of Mining and Metallurgy, London, pp. 173-181.

Poulos, H.G. and Davis, E.H. (1974) Elastic solutions for soil and rock mechanics. Wiley, New York.

Terzaghi, K. (1943) Theoretical soil mechanics. Wiley, New York.

12. **Figures**

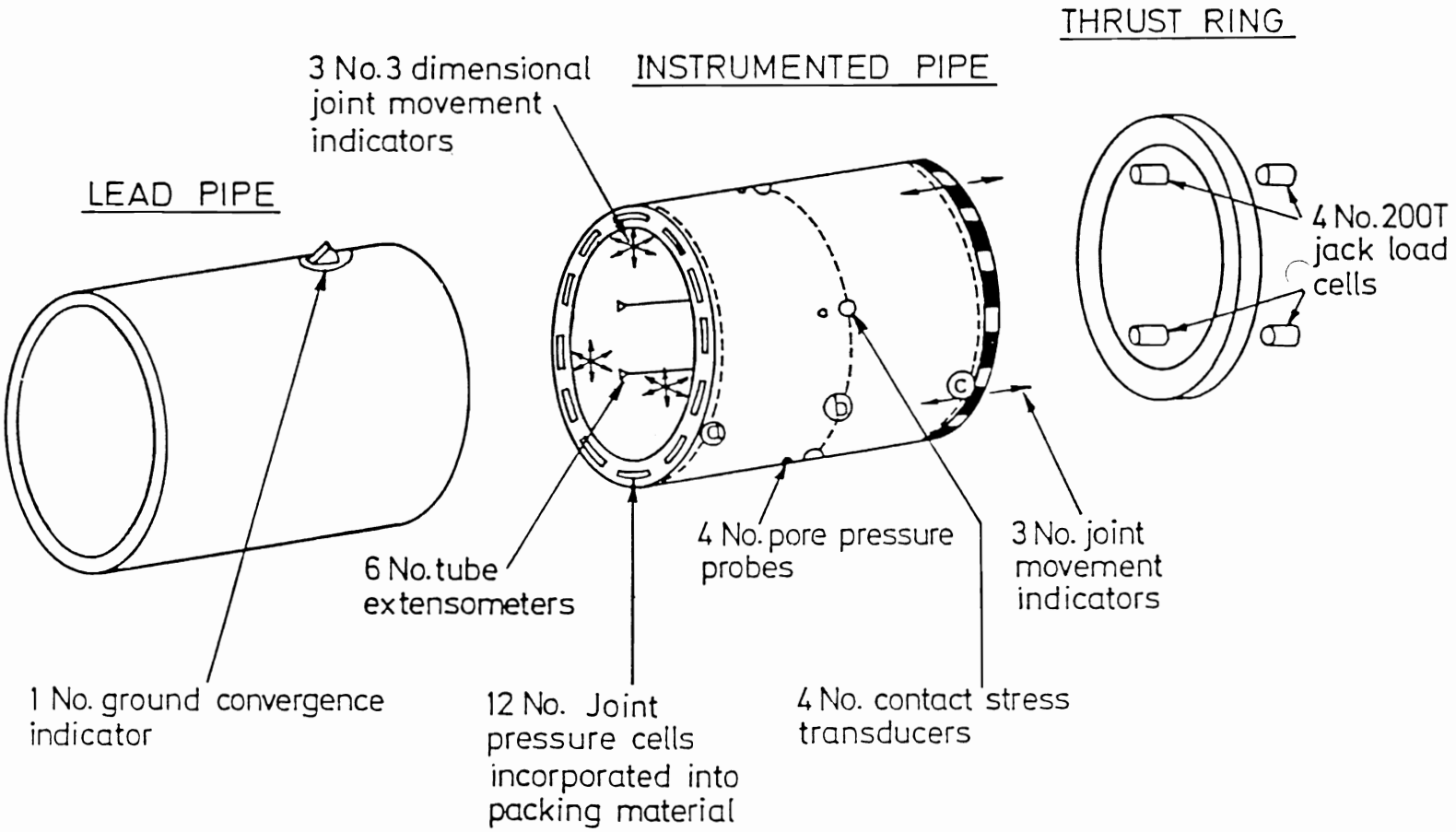

Figure 1.1 Schematic of instrument arrangement (Norris 1992b)

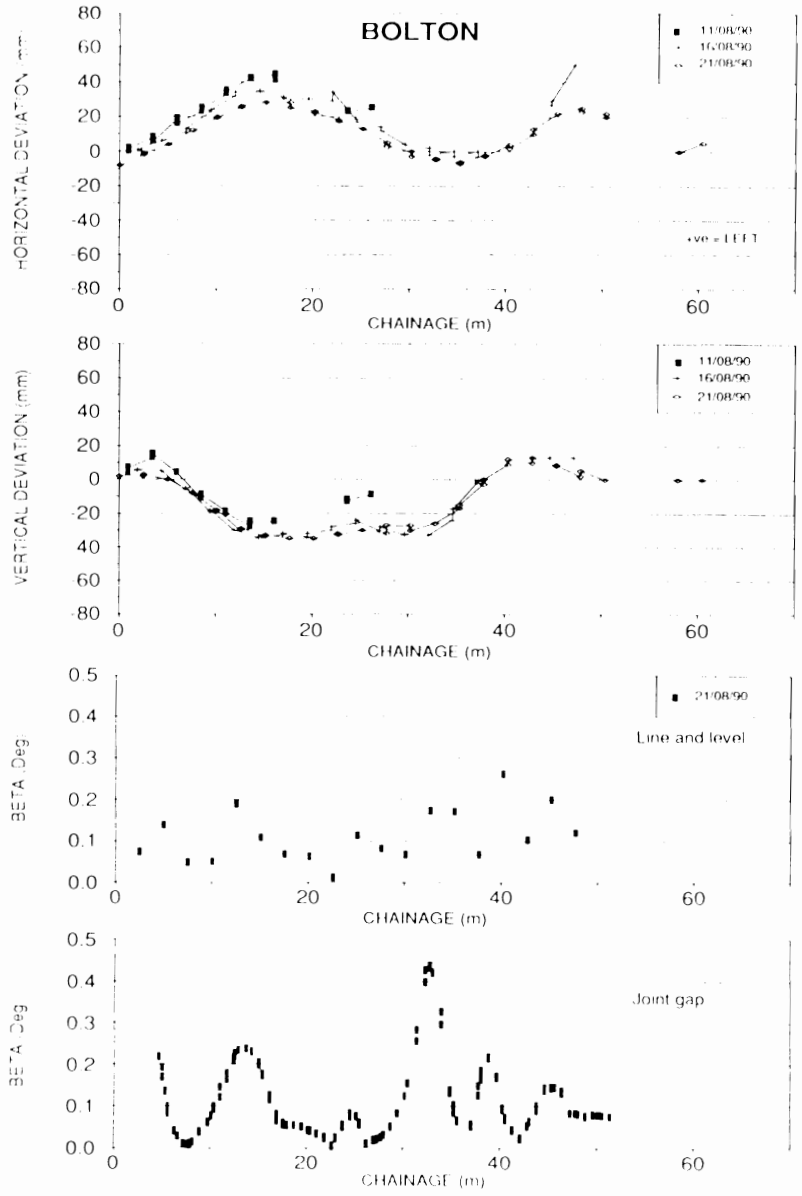

Figure 2.1 Tunnel alignment surveys for scheme 1 (Norris 1992b)

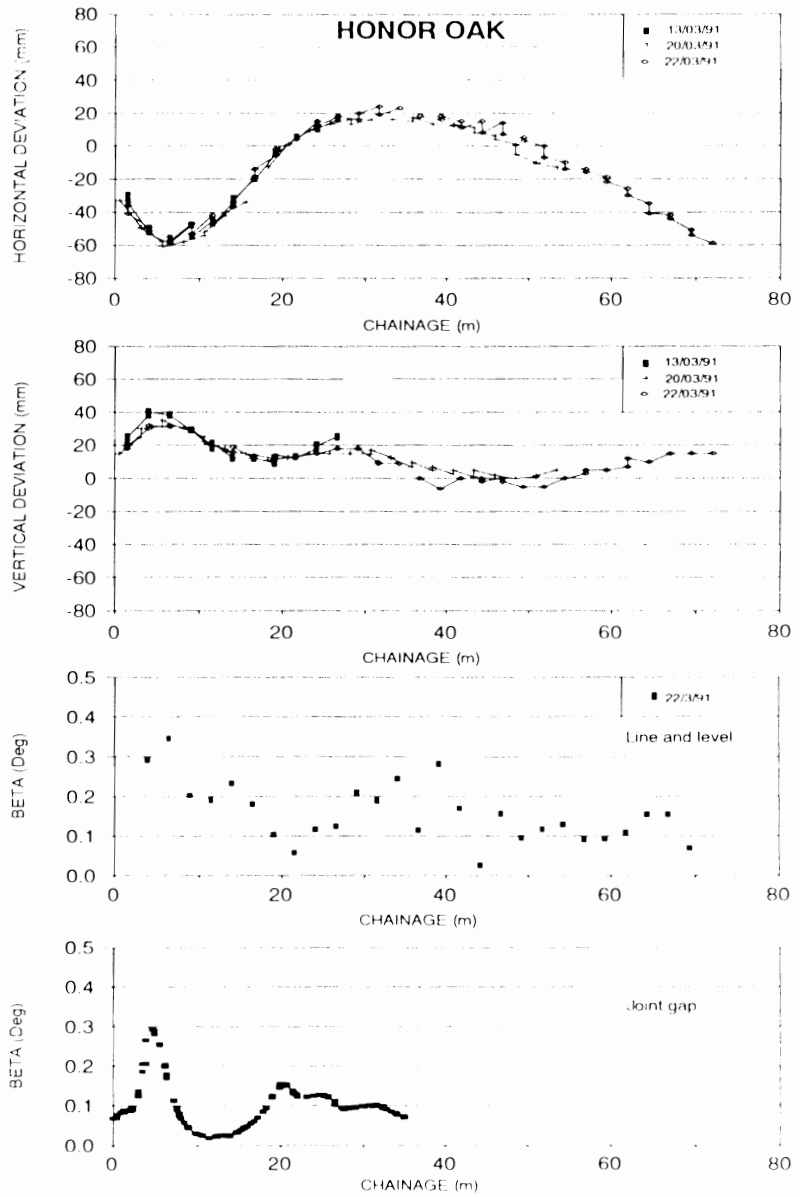

Figure 2.2 Tunnel alignment surveys for scheme 3 (Norris 1992b)

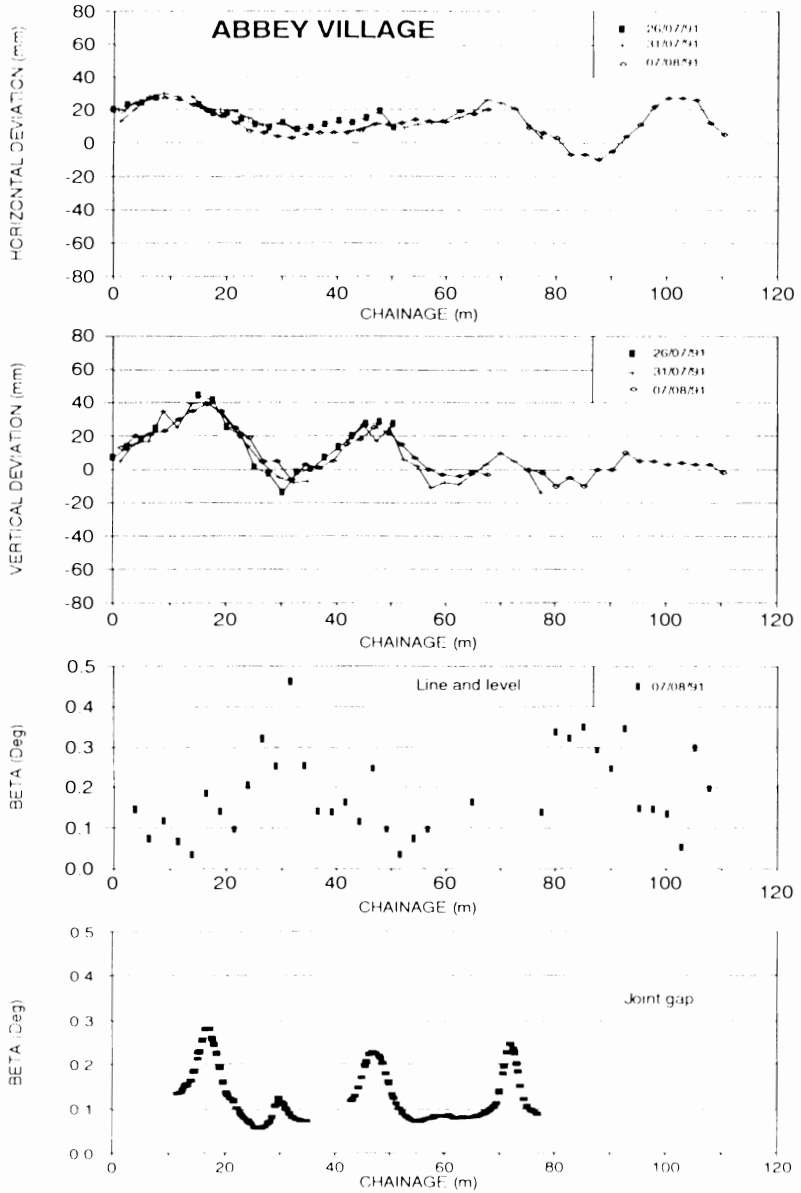

Figure 2.3 Tunnel alignment surveys for scheme 4 (Norris 1992b)

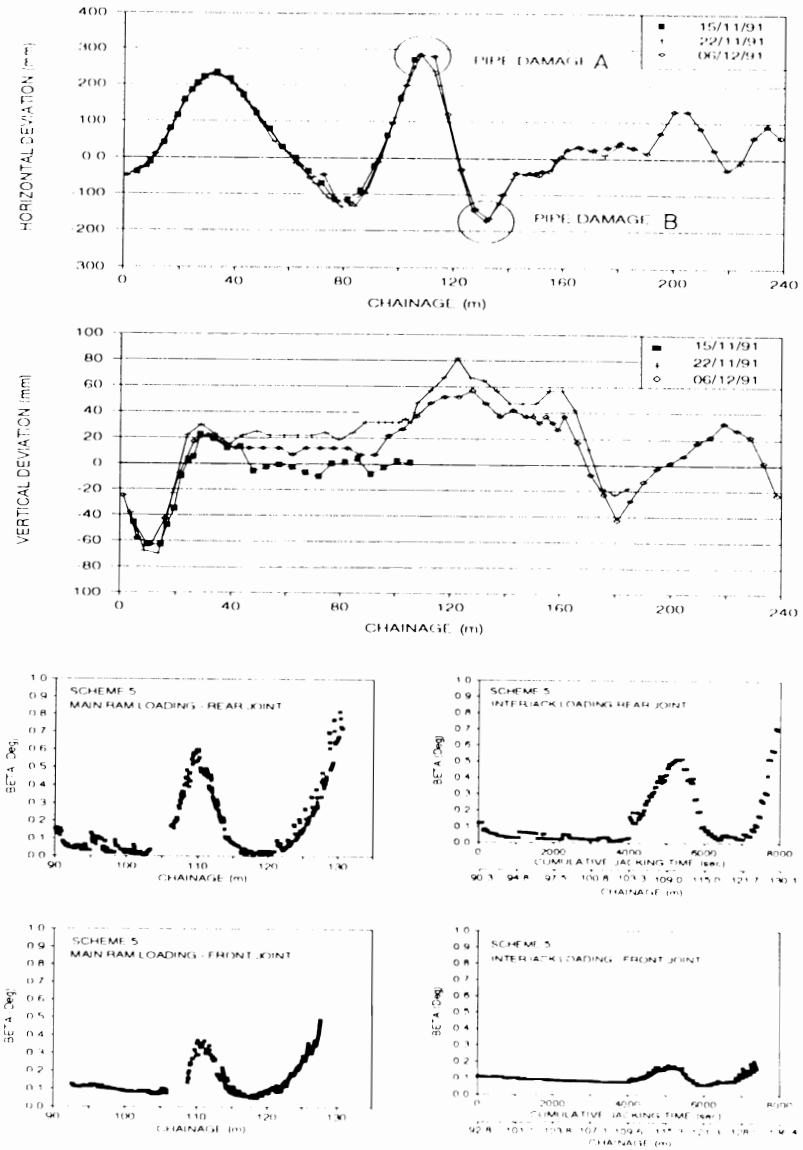

Figure 2.4 Tunnel alignment surveys for scheme 5 (Norris 1992b)

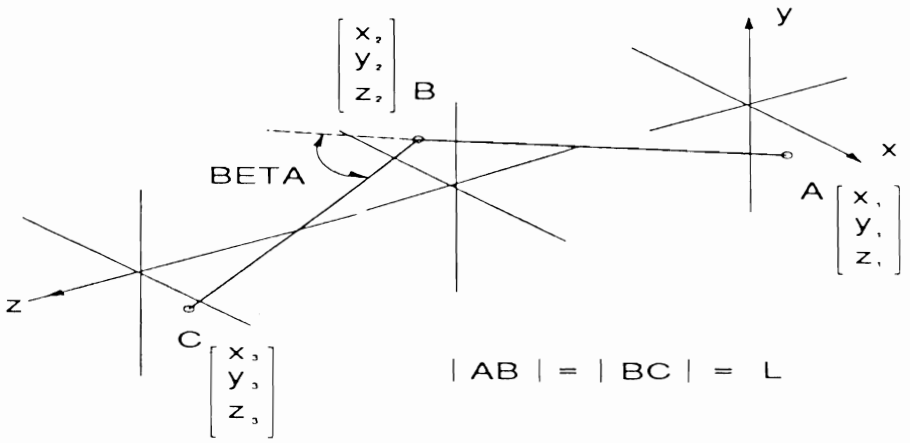

AB and BC represent the centrelines of two successive pipes, with the *x,y,z* co-ordinates being the line error, level error and chainage respectively at the pipe ends.

The direction cosines of AB are

$$l=\frac{x_2-x_1}{L},\quad m=\frac{y_2-y_1}{L},\quad n=\frac{z_2-z_1}{L}$$

likewise the direction cosines of BC are

$$l'=\frac{x_3-x_2}{L},\quad m'=\frac{y_3-y_2}{L},\quad n'=\frac{z_3-z_2}{L}$$

then the misalignment angle ß is given by

$$\cos\beta = l.l' + m.m' + n.n'$$

In practice the values of *z* cannot be obtained sufficiently accurately, but *n* may be determined from the relation

$$l^2+m^2+n^2=1$$

and similarly for *n*'.

Alternatively, for the small deflection angles occurring in practice, the value of ß may be calculated more simply from

$$\sin\beta = \beta(radians) = \frac{\sqrt{(2x_2-x_1-x_3)^2+(2y_2-y_1-y_3)^2}}{L}$$

Figure 2.5 Determination of joint angle ß from line and level surveys

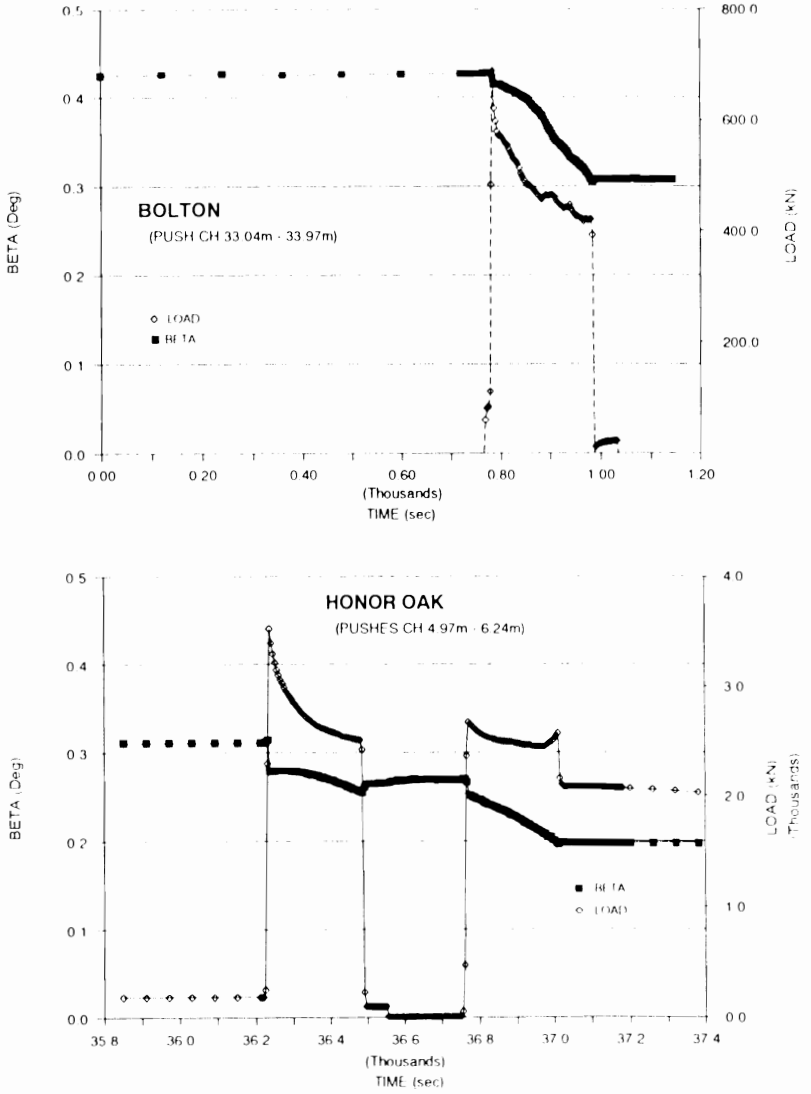

Figure 2.6 Change in ß on application of jacking load, schemes 1 and 3 (Norris 1992b)

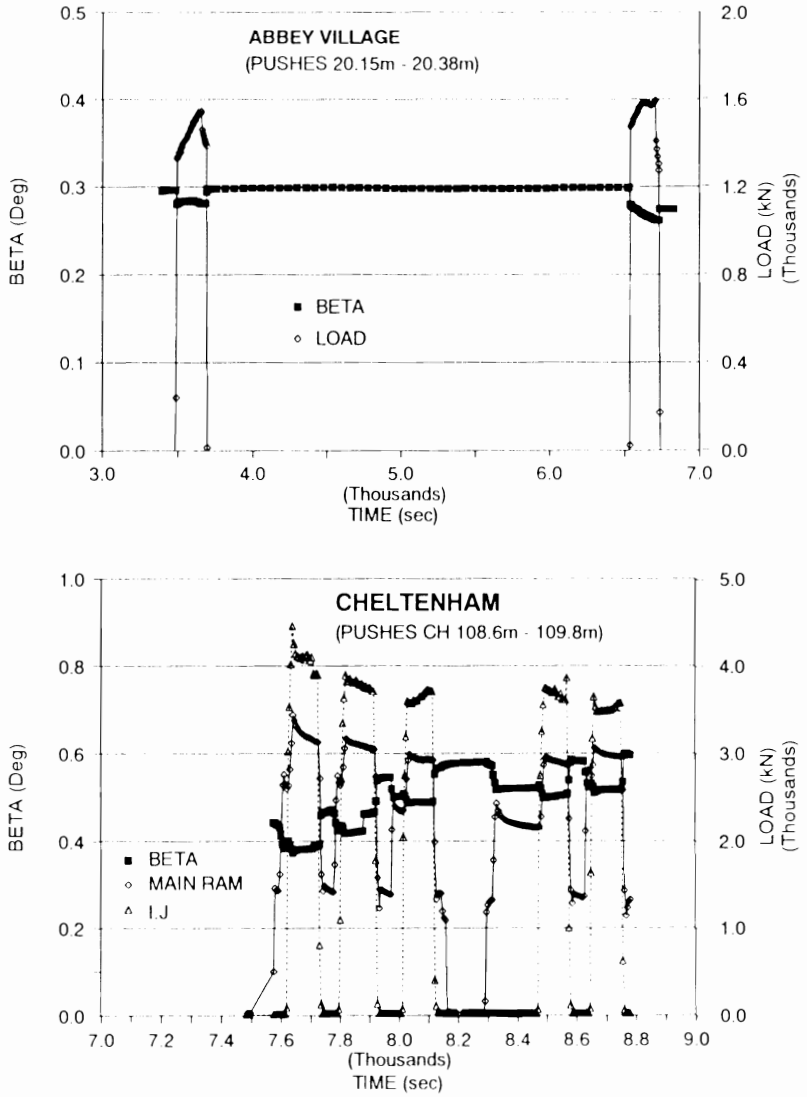

Figure 2.7 Change in ß on application of jacking load, schemes 4 and 5 (Norris 1992b)

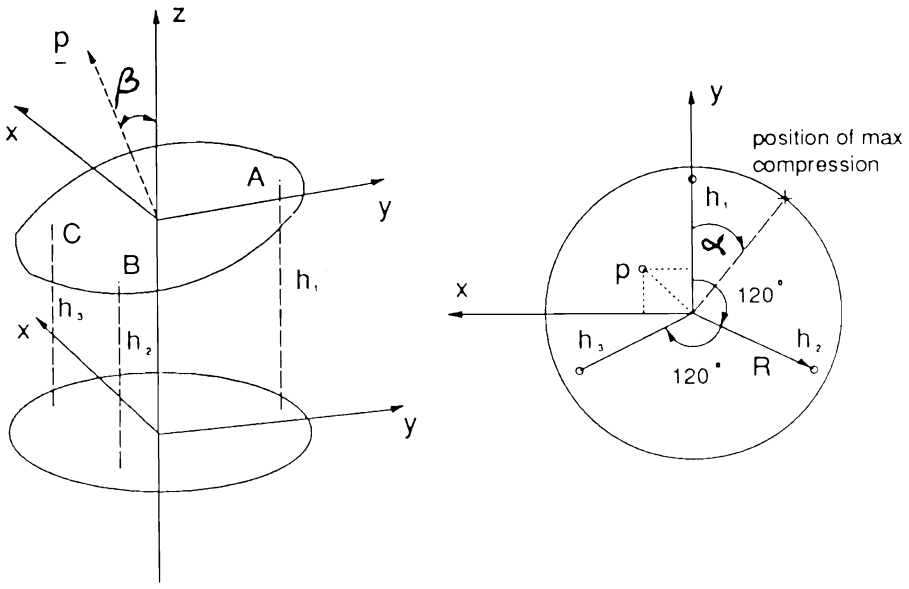

If a joint gap has widths h_1, h_2 and h_3 at three points at a radial distance R and equally spaced around the pipe, it can be shown that

$$\beta = \cos^{-1}\left[\frac{1}{\sqrt{\frac{(h_2-h_3)^2}{3R^2}+\frac{(h_2+h_3-2h_1)^2}{9R^2}+1}}\right]$$

and that

$$\alpha = \tan^{-1}\left\{\frac{\sqrt{3}(h_3-h_2)}{(h_2+h_3-2h_1)}\right\}$$

where ß is the angular rotation at the joint and α is the angular position of the point of maximum compression as shown above.

Note that the second equation always gives two possible solutions for α; the correct one may be identified using the table below.

RANGES FOR α	$h_3 > h_2$	$h_3 < h_2$
$h_2 + h_3 > 2h_1$	0° - 90°	270° - 360°
$h_2 + h_3 < 2h_1$	90° - 180°	180° - 270°

Figure 2.8 Deflections of an instrumented joint (Norris 1992b)

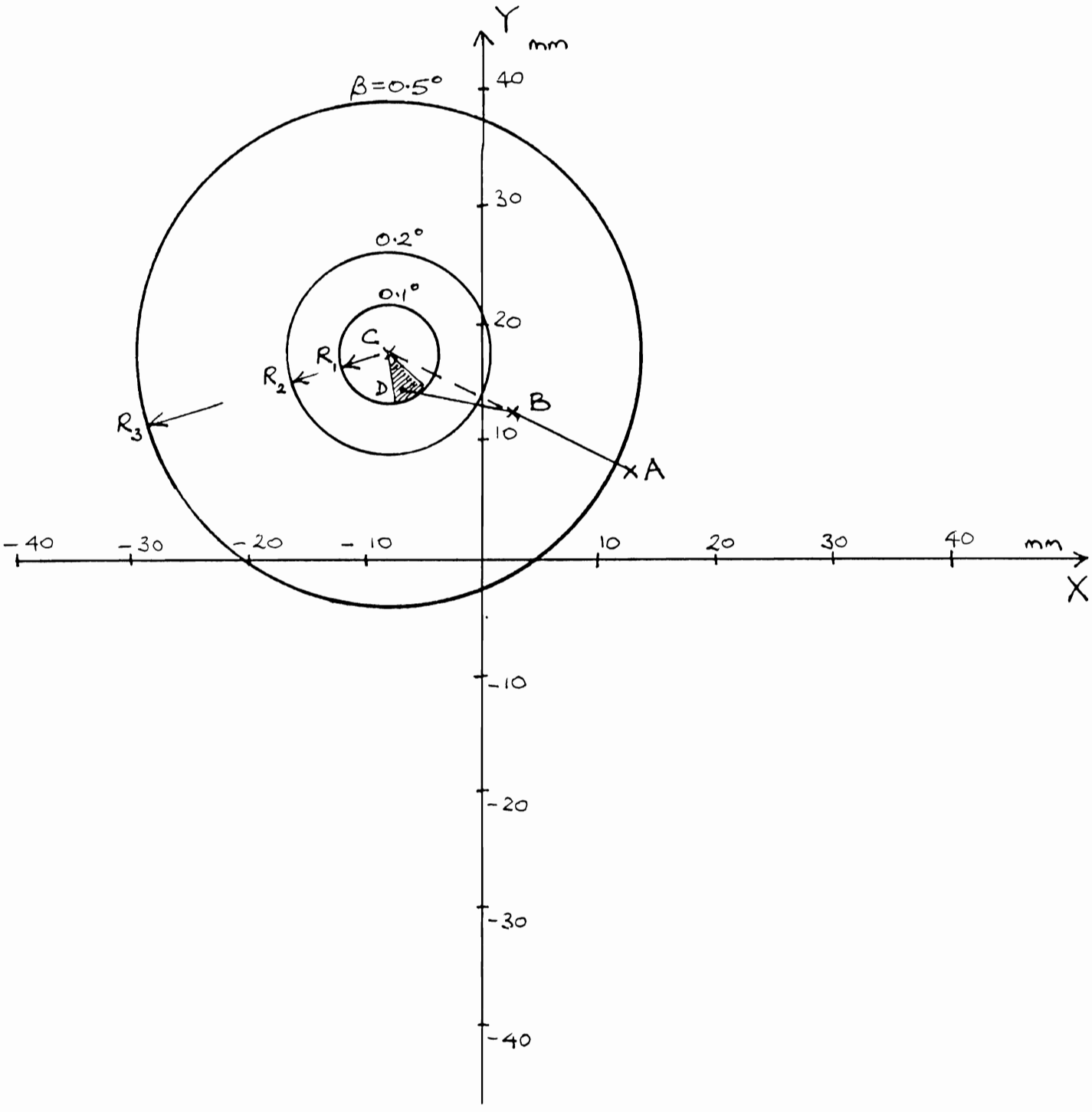

Figure 2.9 Control diagram for pipe jack alignment

In cohesive soils, the pressure σ_T required to maintain stability of the tunnel face is given by

$$\sigma_T > \gamma(C+D/2) - T_c.s_u$$

where γ = unit weight of soil, s_u= undrained strength of soil
and T_c= stability ratio - see plot below (Atkinson and Mair 1981).
In pipe jacked tunnels the unsupported length P is usually small or zero, and P/D=0.
e.g. for γ = 20 kN/m^3, C = 4m, D = 2m, the plot gives T_c = 8
hence σ_T = 100 - 8.s_u kPa
and for s_u > 12.5 kPa, no support is needed.

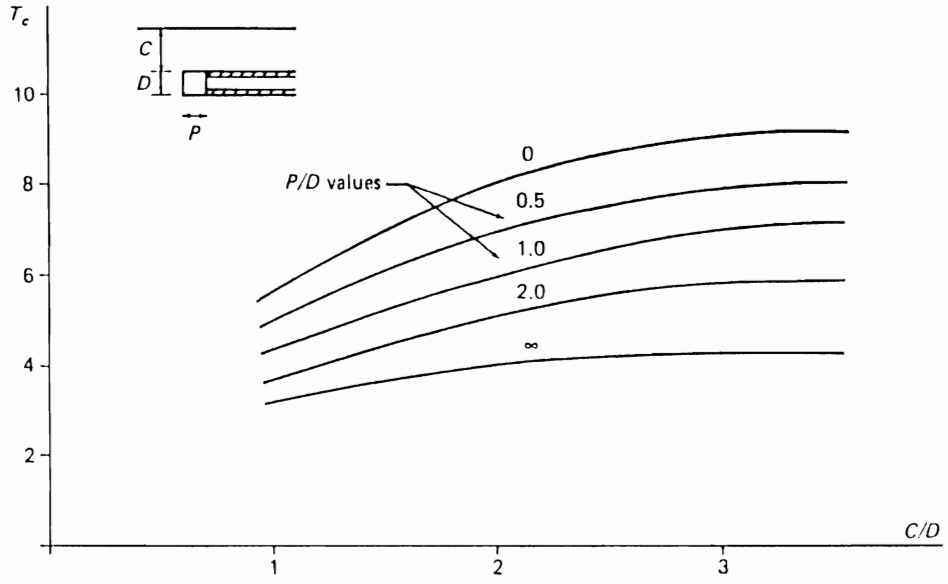

To prevent blow-out due to excessive face pressure,

$$\sigma_T < \gamma(C+D/2) + T_c.s_u$$

In both cases, a factor of safety of 1.5 to 2.0 on s_u is needed to limit heave and settlement in soft clays, for example see below (Mair 1987).
In this case, say γ = 20 kN/m^3, D = 2.0m, s_u = 10 kPa, then $\gamma D/s_u$ = 4.
For C/D = 2.0, σ_T must lie between 6 and 14 times s_u, i.e. between 60 and 140 kPa.

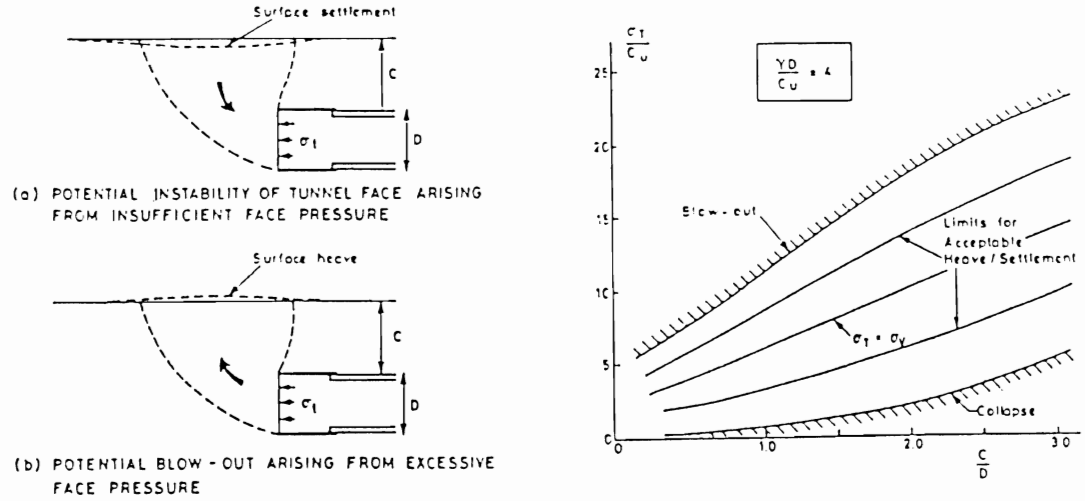

Figure 3.1 Face stability in cohesive soils

For the tunnel behind the shield, the conditions correspond to the case in Figure 3.1 of P/D $\rightarrow \infty$. The equation for calculating the support pressure required to prevent collapse is as before

$$\sigma_T = \gamma(C+D/2) - T_c.s_u$$

which may be re-arranged to give

$$\frac{\sigma_T}{s_u} = \frac{\gamma.D}{s_u}(C/D+1/2) - T_c$$

This gives rise to plots shown below. Again, values of σ_T less than zero indicate that the tunnel is stable without any support pressure. Note that for microtunnels $\gamma D/s_u << 1.0$ in most cases, and the tunnel bore will normally be stable.

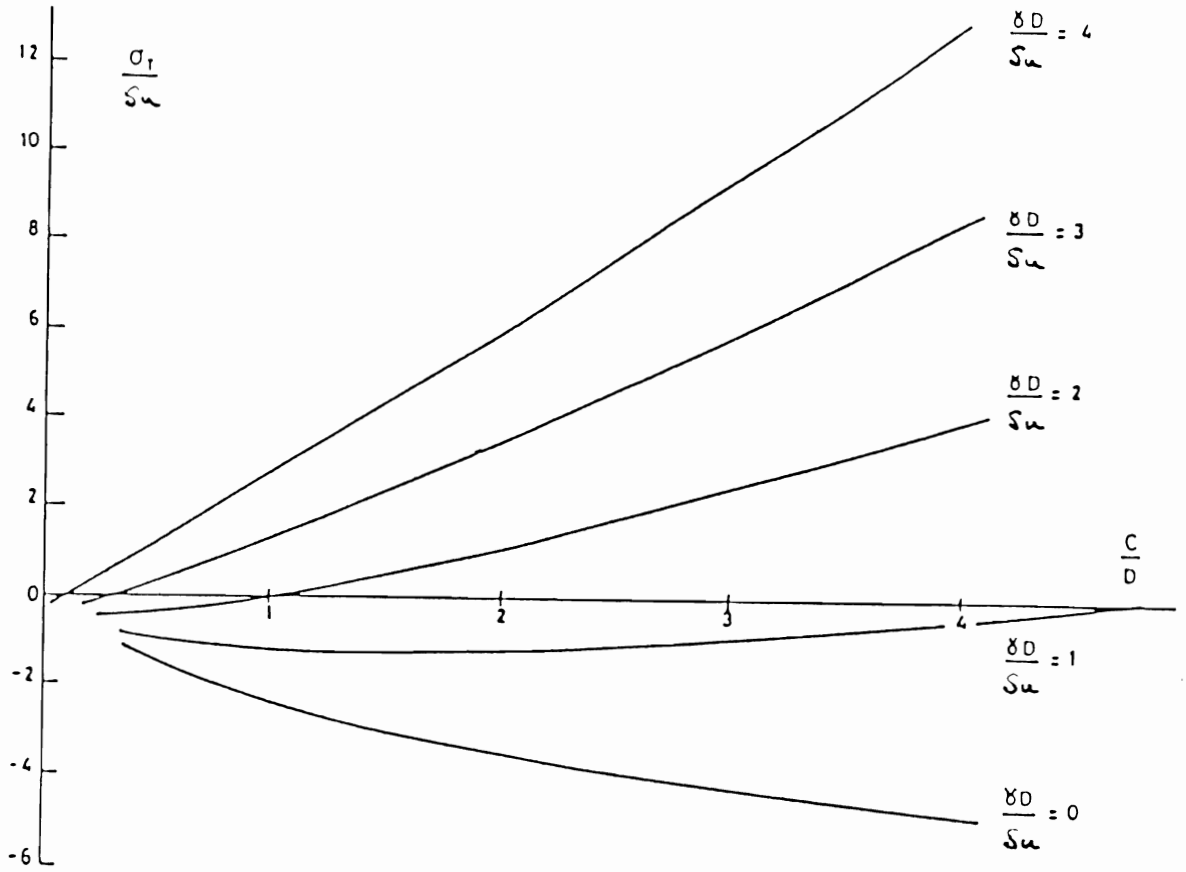

For example, for C/D = 2, and $\gamma D/s_u = 4$, from Figure 3.1 $T_c = 4$
then $\sigma_T/s_u = 4 \times 2.5 - 4 = 6$, or directly from plot above.
i.e. for $s_u = 10$ kPa, $\sigma_T = 60$ kPa.

Figure 3.2 Tunnel stability in cohesive soils

For tunnels in cohesionless soil without a surcharge on the surface, the required support pressure σ_T is independent of the cover depth and is given by

$$\sigma_T = \gamma . D . T_\gamma$$

where T_γ is the stability number given by the plot below; it is a function only of ϕ, the friction angle for the soil.

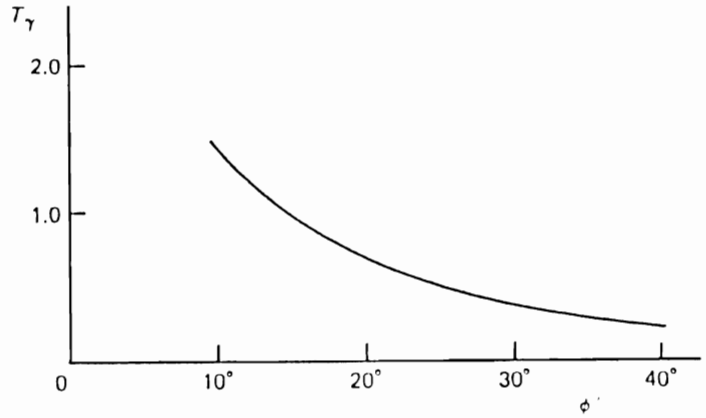

For example, if γ = 18 kN/m^3, D = 1.6m, and ϕ = 35°,
then from the plot T_γ = 0.3 and σ_T = 18 x 1.6 x 0.3 = 8.6 kPa

Alternatively, if the tunnel is at shallow depth and a large surcharge σ_s acts on the surface, the weight of soil may be neglected and then

$$\sigma_T = \sigma_s . T_s$$

with the stability number T_s as given in the plot below.

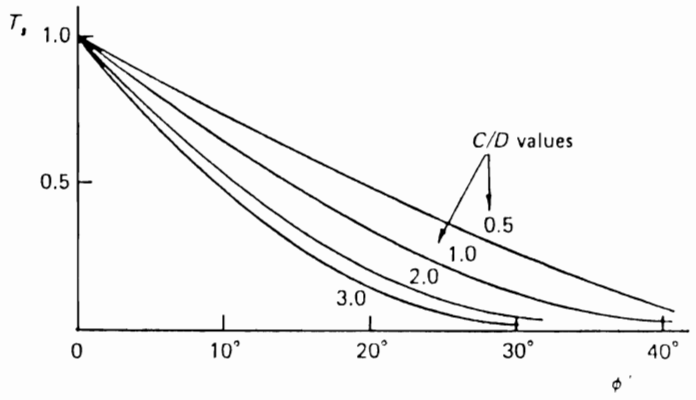

Note that both solutions apply to dry soil. Water pressure, if present, must be added to σ_T and the buoyant weight of soil used in the first equation.

Figure 3.3 Tunnel stability in cohesionless soils

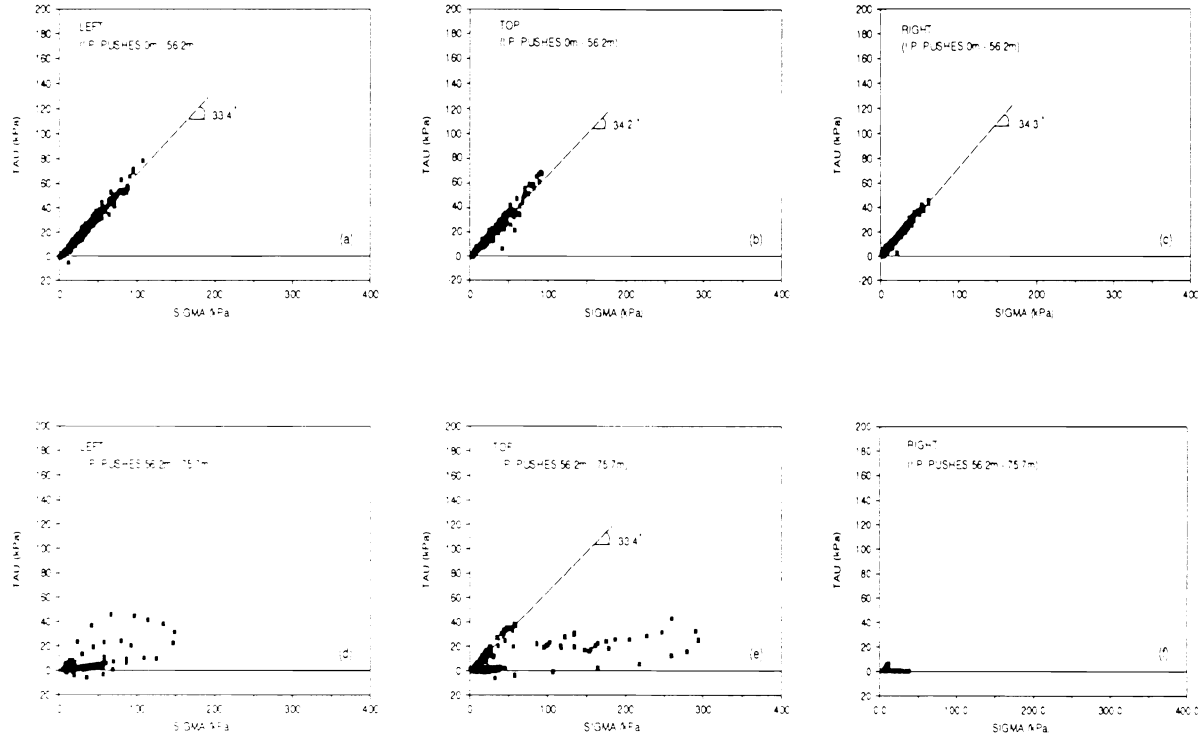

Figure 3.4 Shear stress/total radial stress relations from scheme 4; prior to lubrication (a-c) and during lubrication (d-f) (Norris 1992b)

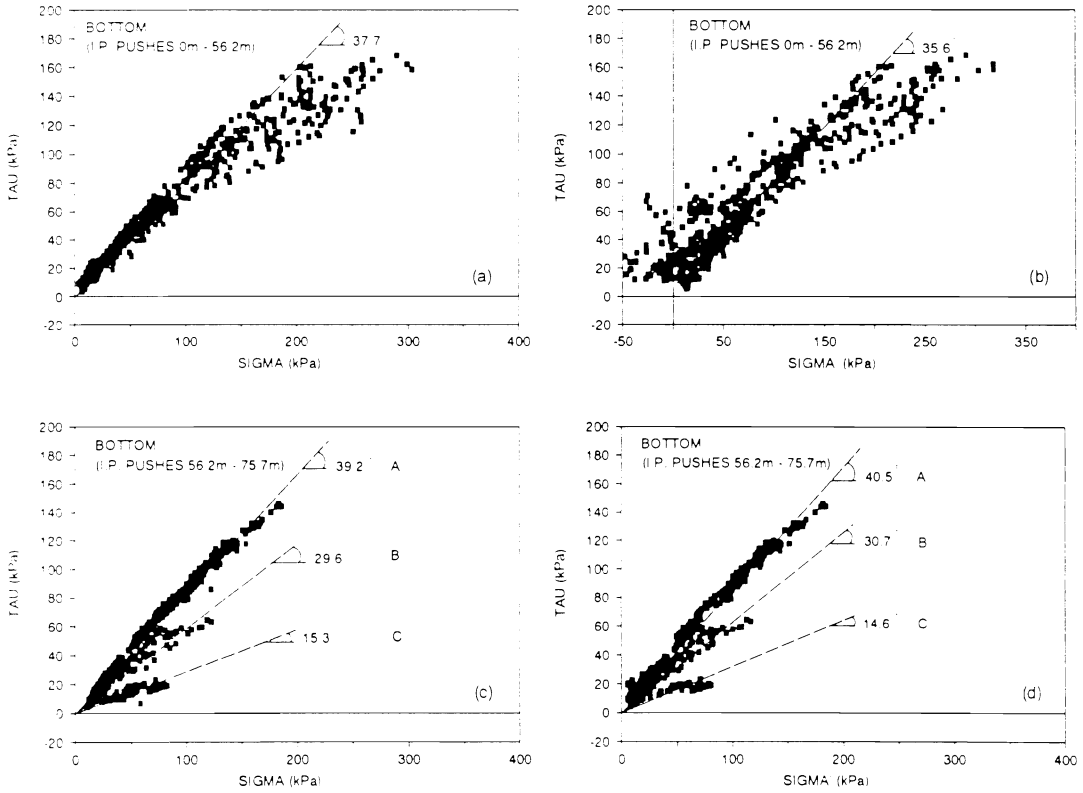

Figure 3.5 Shear stress/radial stress relations from scheme 4; total and effective stress responses on the bottom of the pipe prior to lubrication (a & b) and during lubrication (c & d) (Norris 1992b)

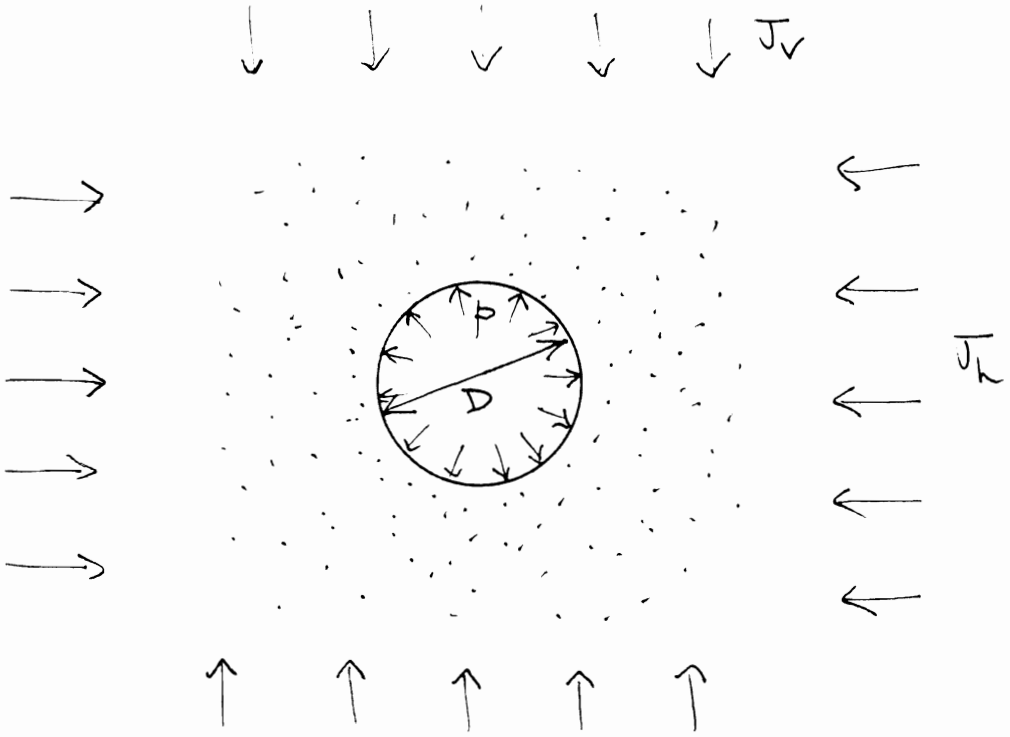

For initial vertical and horizontal stresses in the ground σ_v and σ_h, the reduction in vertical diameter of the tunnel bore due to elastic stress relief is given by

$$\delta_v = \frac{(1-\nu^2)}{E} D(3\sigma_v + \sigma_h)$$

and similarly the reduction in the horizontal diameter is given by

$$\delta_h = \frac{(1-\nu^2)}{E} D(3\sigma_h + \sigma_v)$$

where E and ν are the Young's modulus and Poisson's ratio for the soil.

If an internal support pressure p is applied, the symmetrical increase in diameter is given by

$$\delta_p = \frac{(1+\nu)}{2E} pD$$

For example, in scheme 5, D = 1.45m, σ_v = 5.4 x 19 = 103 kPa
take K_0 = 1 - sinϕ = 0.47, hence σ_h = 0.47 x 103 = 48 kPa
taking E = 100 MPa, ν =0.2, gives δ_v = 5.0mm
and for p = 50 kPa, δ_p = 0.44mm
thus total maximum inward movement = 4.6mm, and initial overbreak of 20mm on diameter would not be closed.

Figure 3.6 Calculation of ground closure

For a tunnel with initial vertical and horizontal stresses in the ground

$$p_z = \sigma_v = \gamma.z$$

$$p_x = \sigma_h = N.p_z$$

the radial stress σ_r at the tunnel surface is zero and the maximum value σ_{max} of the circumferential stress σ_c may be obtained from the figure below for the appropriate value of N. Note that the largest values occur for $N > 1$, i.e. in beds of heavily overconsolidated clay.

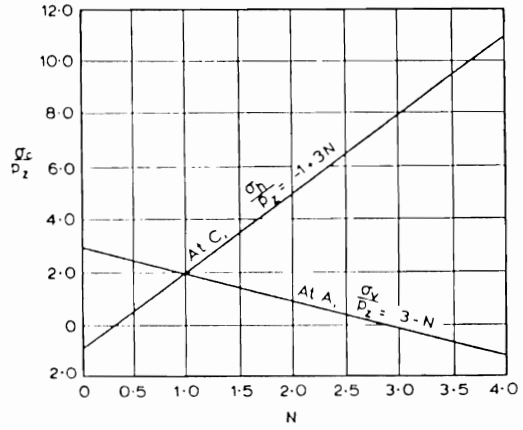

Circumferential principal stress at surface of circular tunnel as function of N (Terzaghi and Richart, 1952).

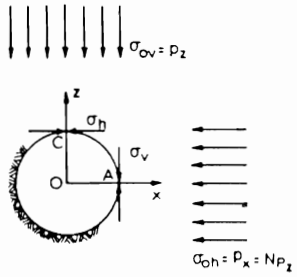

If there is an internal pressure in the tunnel (e.g. due to bentonite lubricant) of $\sigma_T = p$, then this causes stresses at the tunnel surface of

$$\sigma_\theta = -p, \qquad \sigma_r = +p$$

For local yielding to occur,

$$\sigma_\theta - \sigma_r = 2s_u$$

$$\therefore (\sigma_c - p) - p = \sigma_c - 2p = 2s_u$$

Figure 3.7 Conditions for local yielding at the tunnel surface

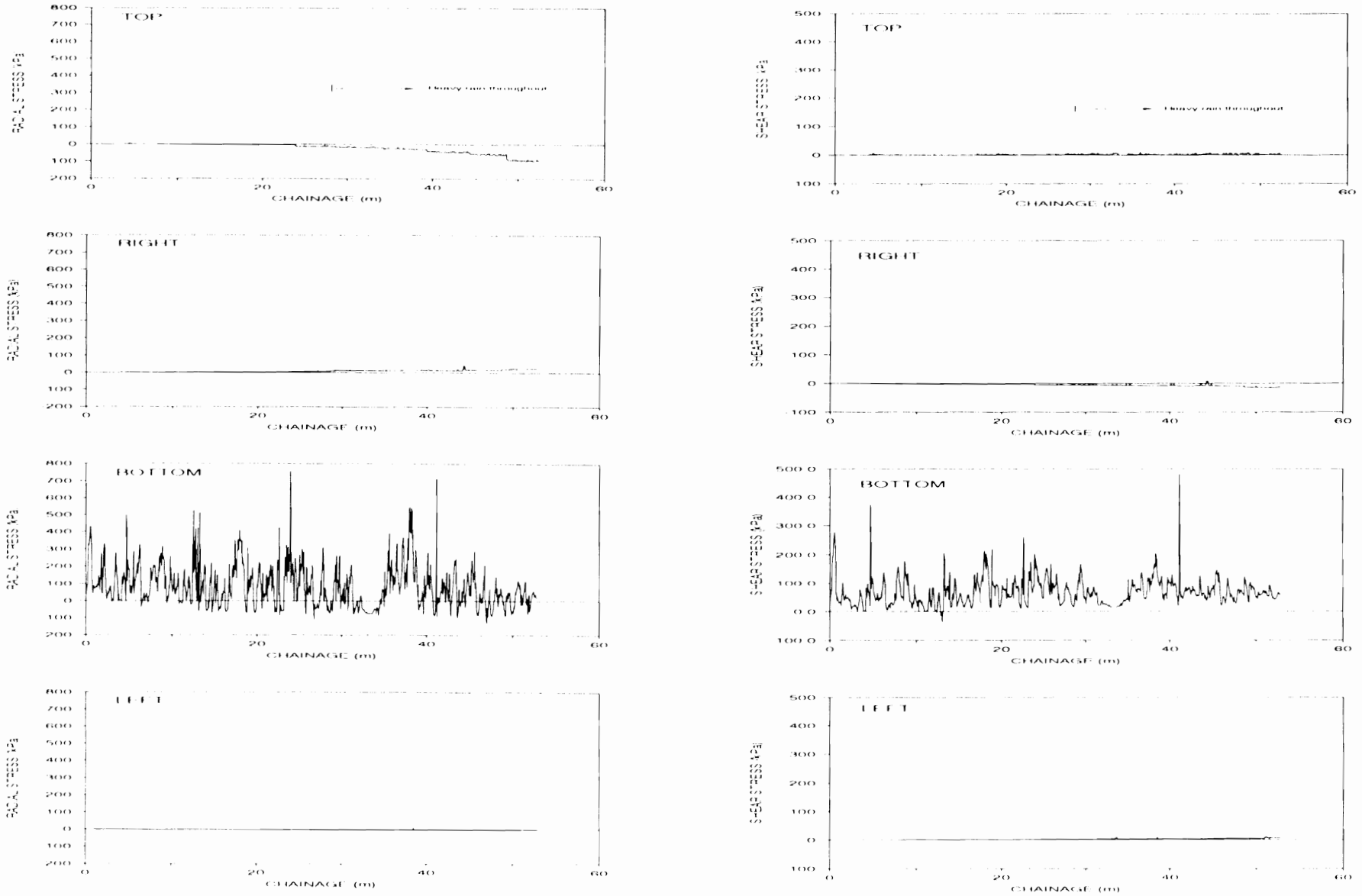

Figure 4.1 Variations in total radial and interface shear stresses in scheme 1 (Norris 1992b)

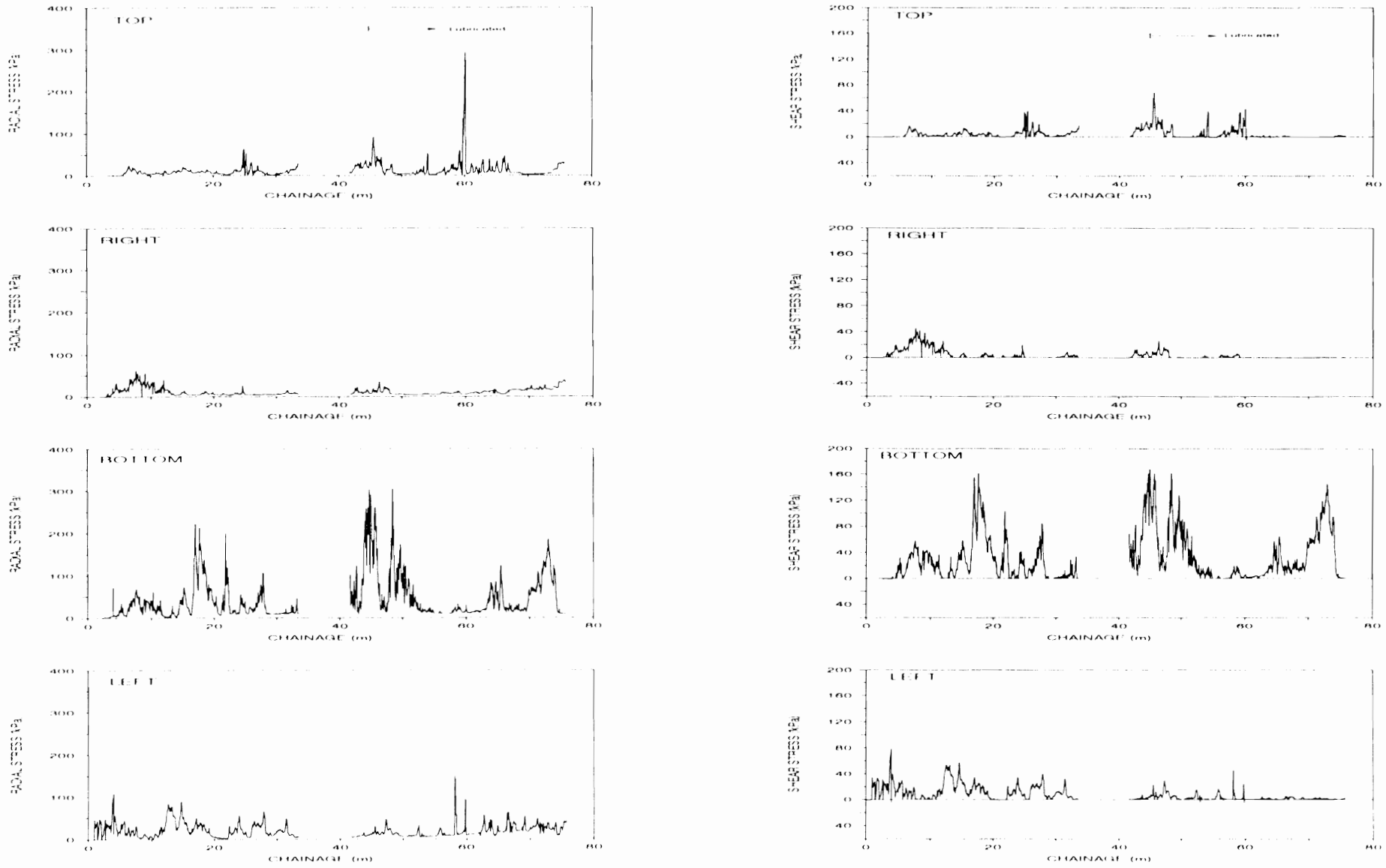

Figure 4.2 Variations in total radial and interface shear stresses in scheme 4 (Norris 1992b)

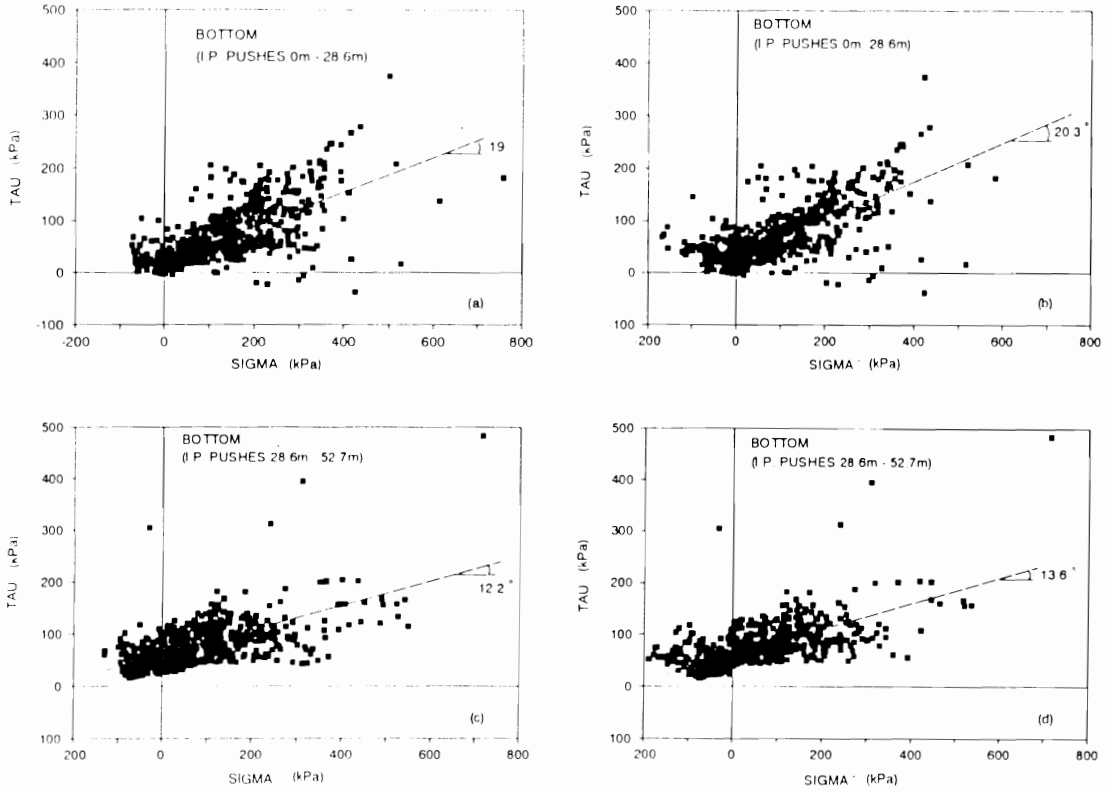

Figure 4.3 Shear stress/radial stress relations from scheme 1; total and effective stress responses prior to heavy rain (a & b), and after wetting (c & d) (Norris 1992b)

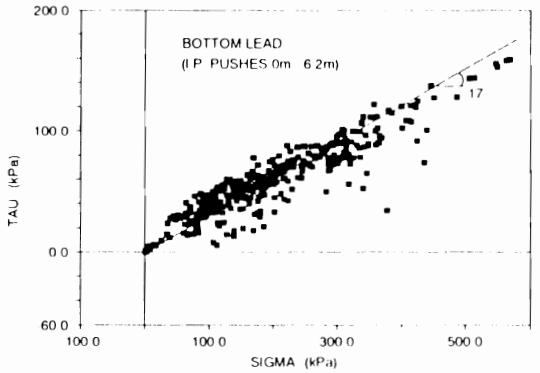

Figure 4.4 Shear stress/total radial stress relation from scheme 2 (Norris 1992b)

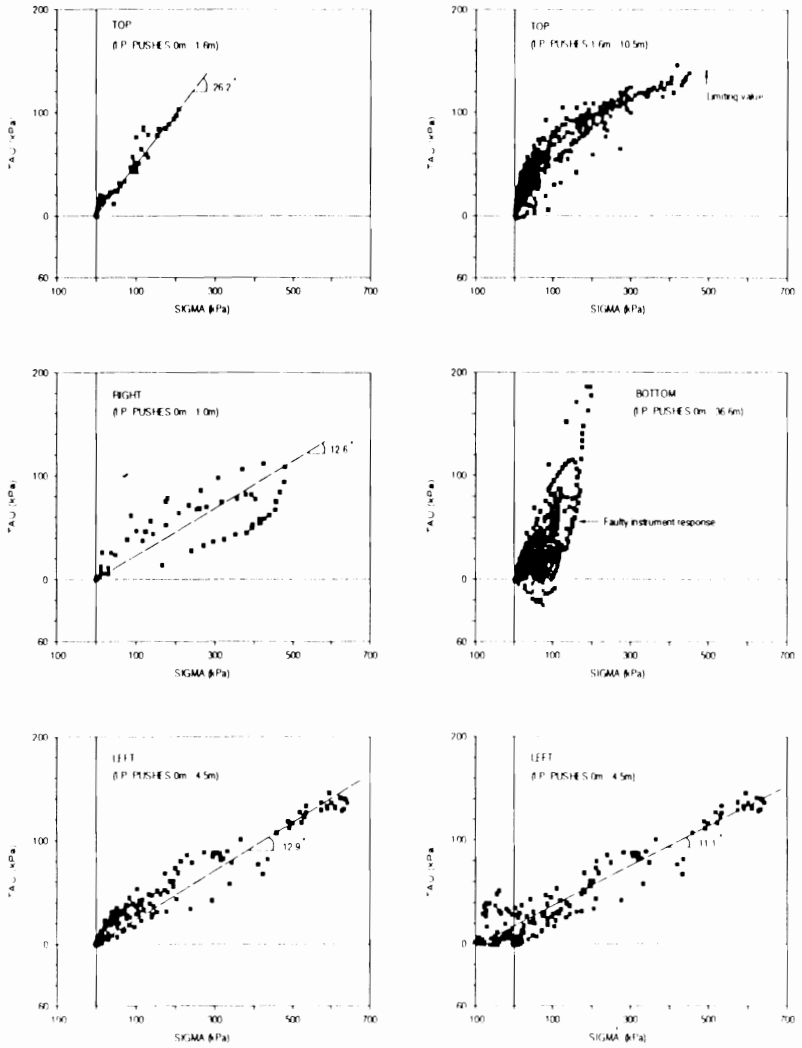

Figure 4.5 Shear stress/radial stress relations from scheme 3 (Norris 1992b)

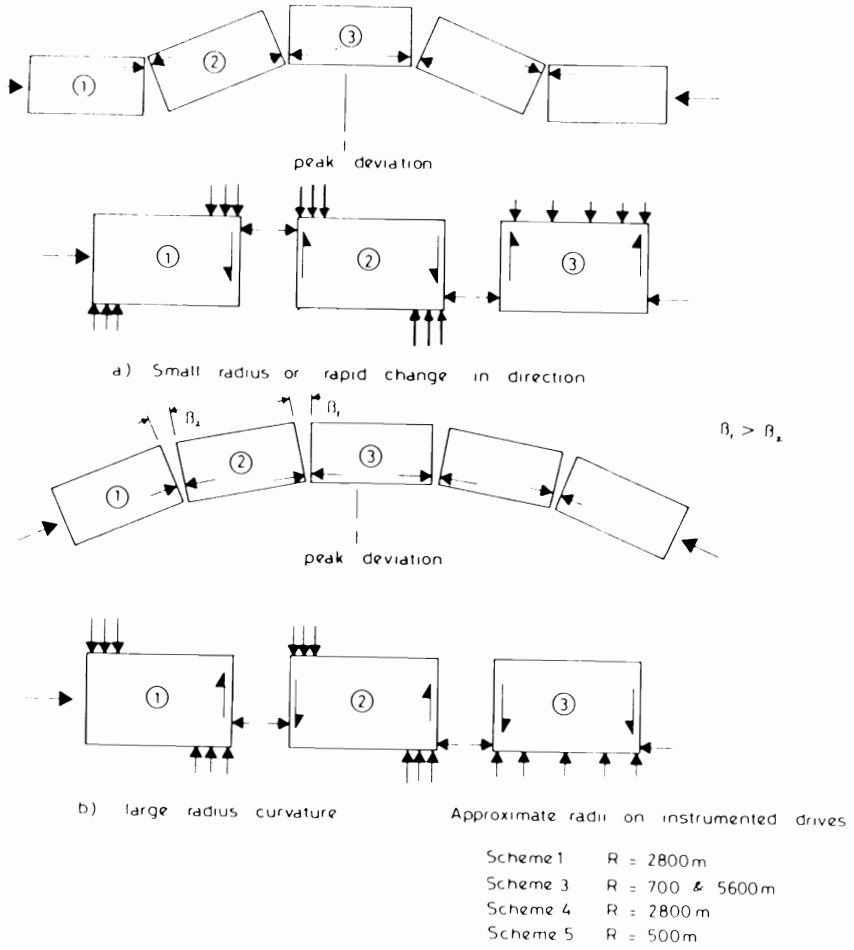

Figure 4.6 Theoretical misalignment forces (Norris 1992b)

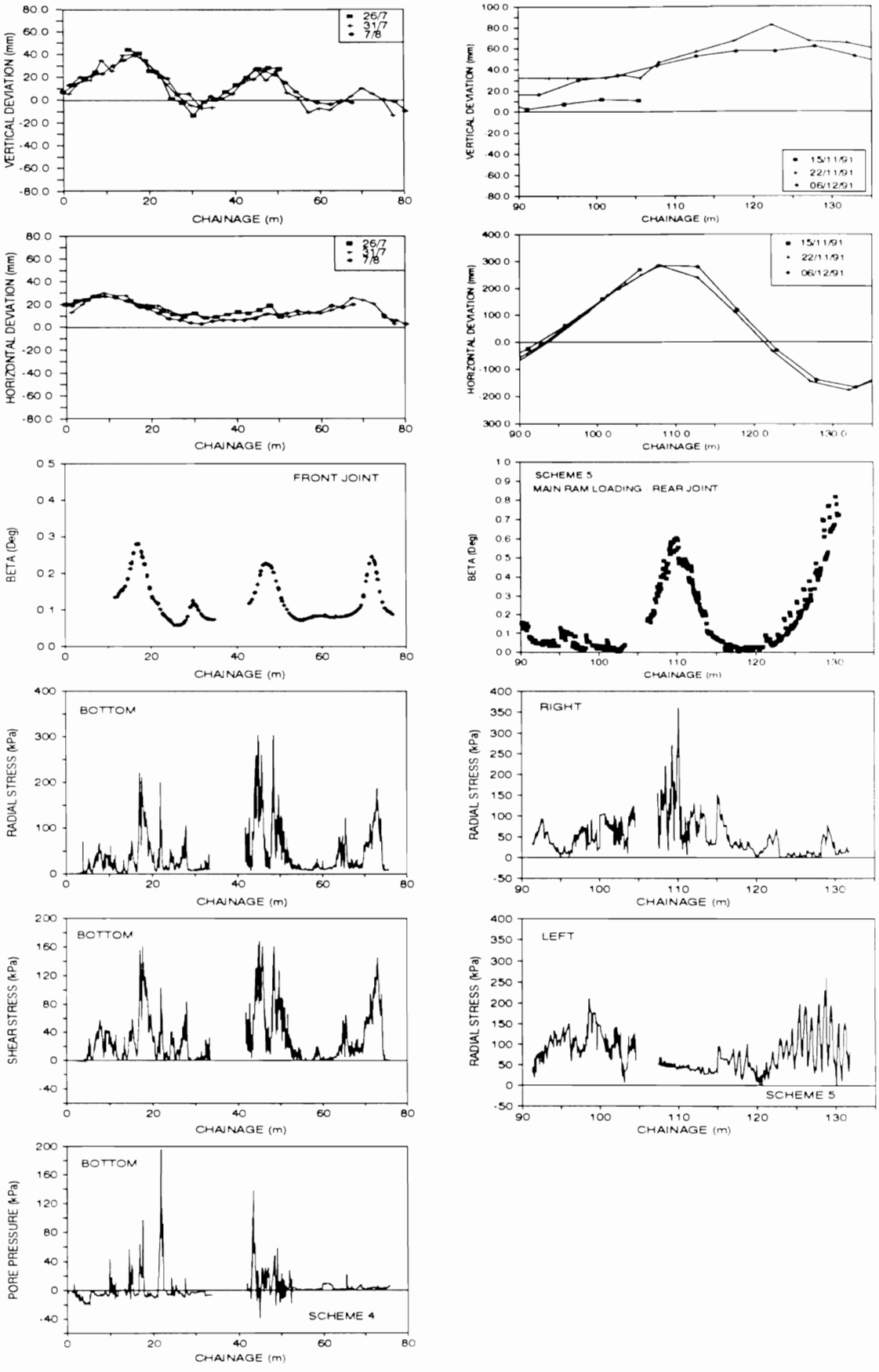

Figure 4.7 Comparison of tunnel alignment data and local interface stresses (Norris 1992b)

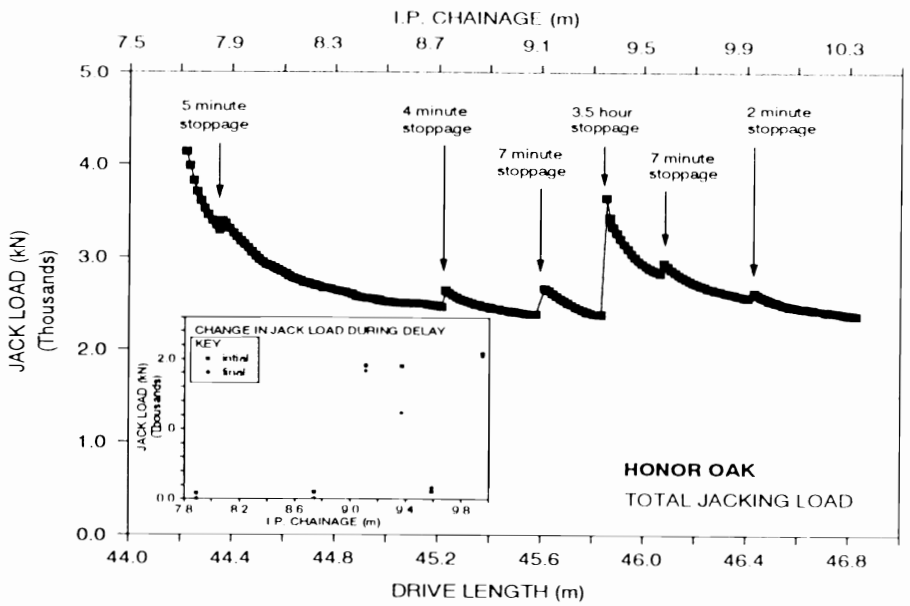

Figure 4.8 Changes in jacking load during stoppages on scheme 3 (Norris 1992b)

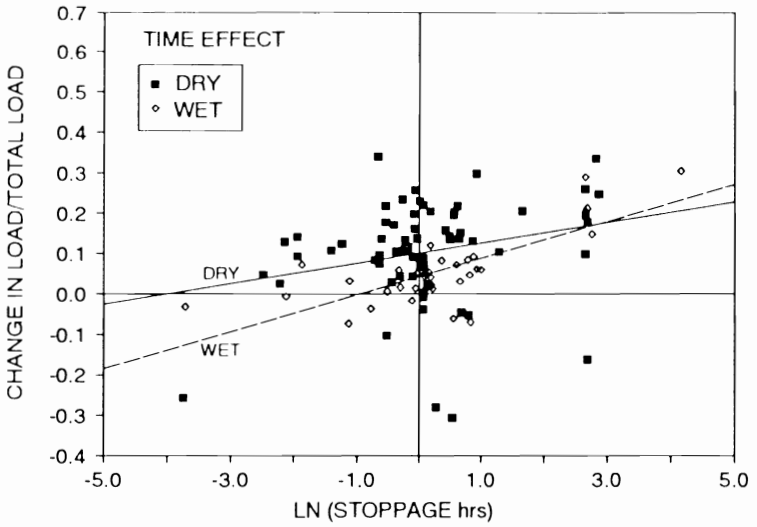

b) Scheme 1

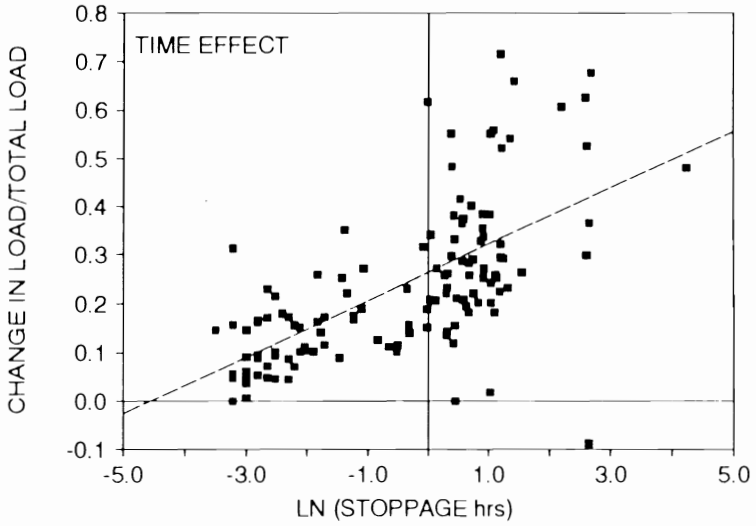

a) Scheme 3

Figure 4.9 Time factors for schemes 1 & 3 (Norris 1992b)

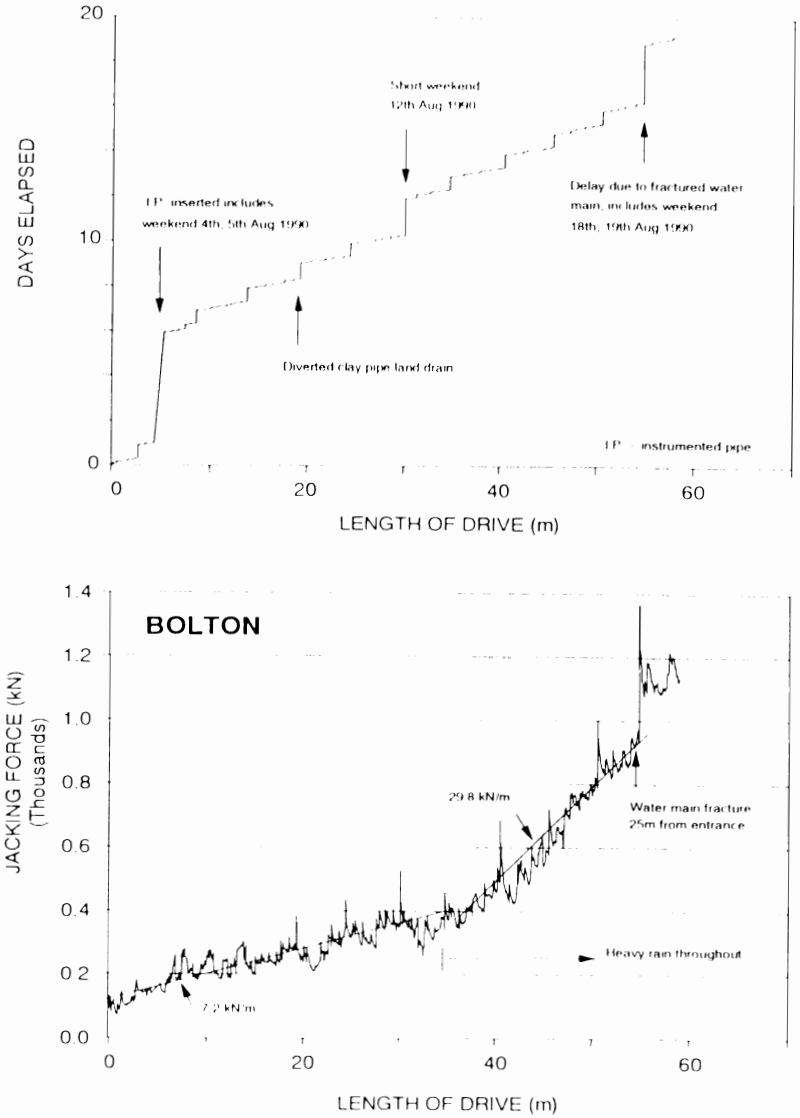

Figure 5.1 Jacking records for scheme 1 (Norris 1992b)

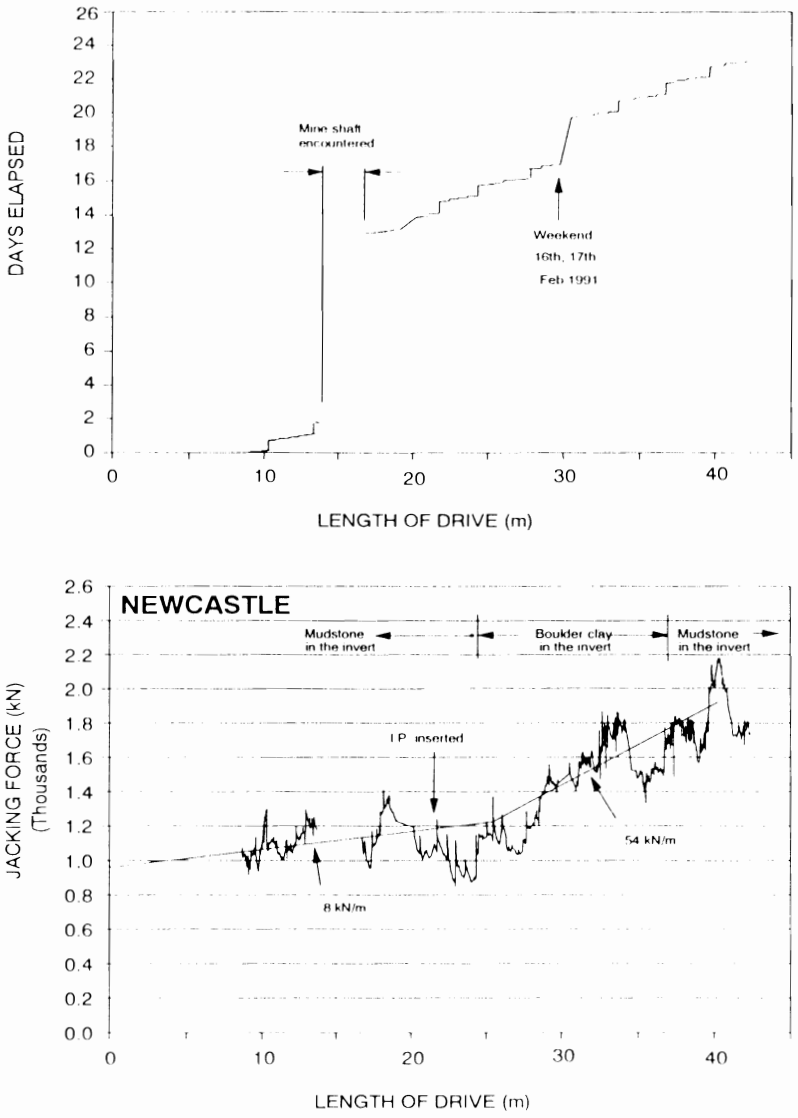

Figure 5.2 Jacking records for scheme 2 (Norris 1992b)

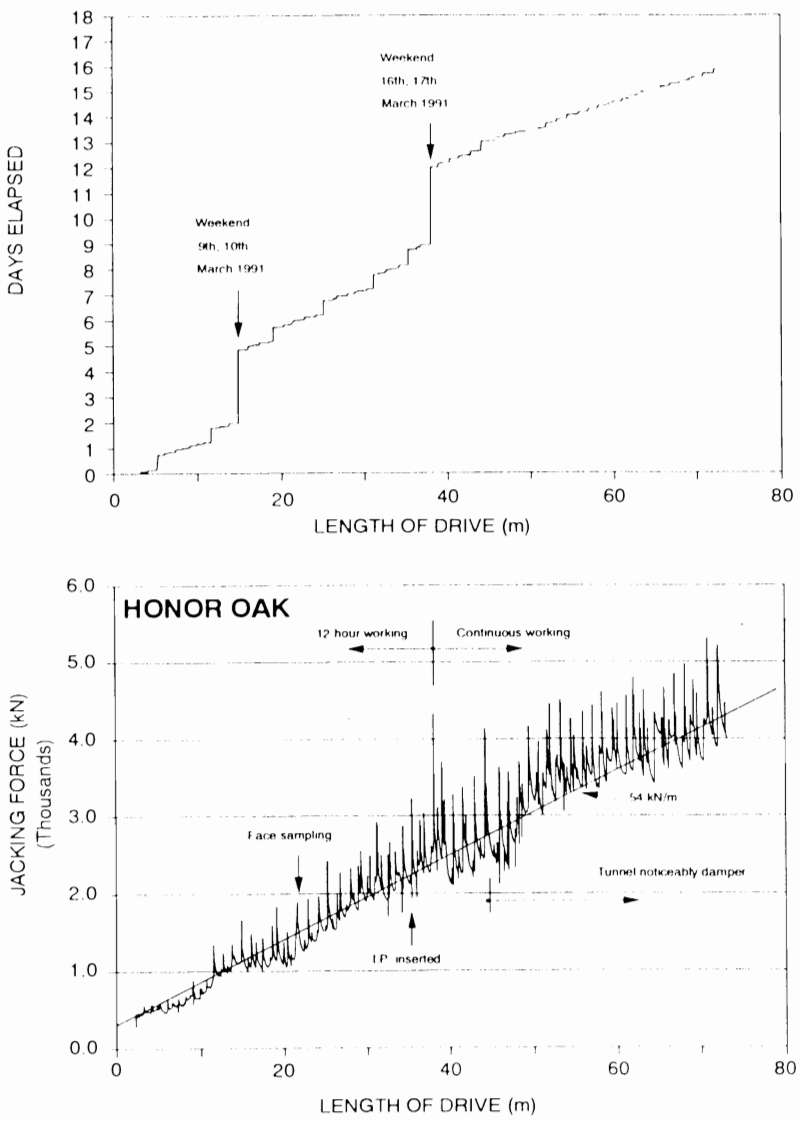

Figure 5.3 Jacking records for scheme 3 (Norris 1992b)

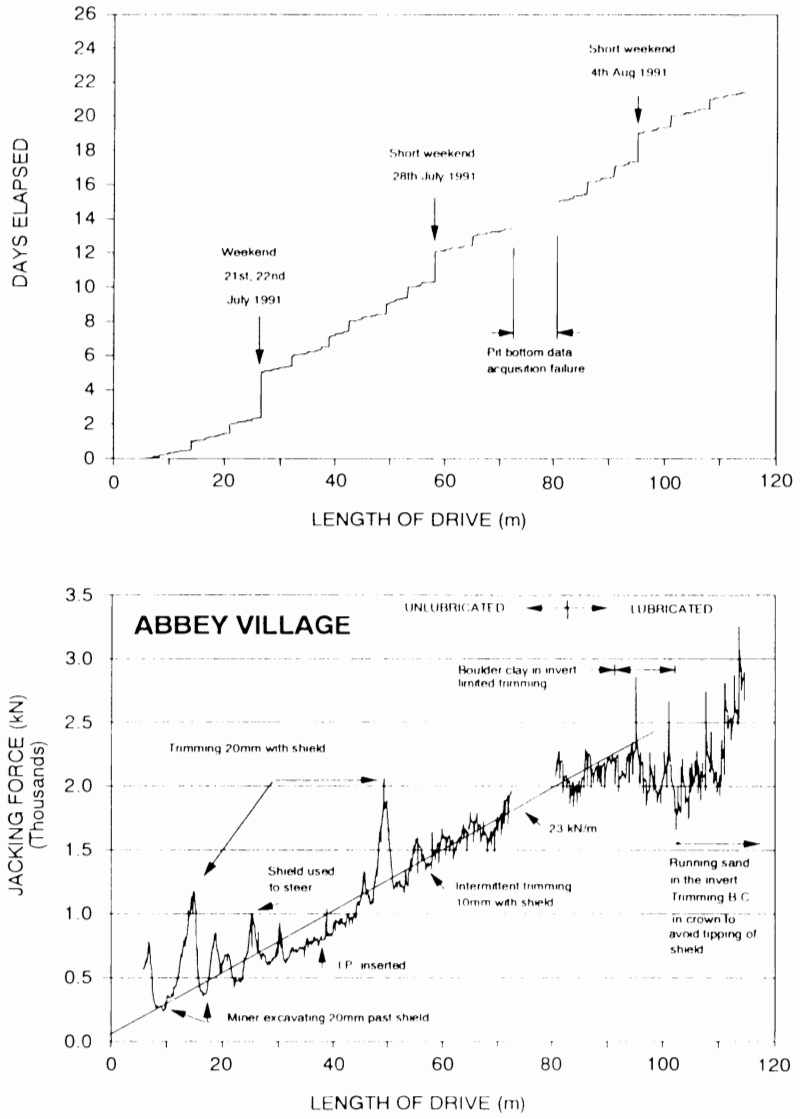

Figure 5.4 Jacking records for scheme 4 (Norris 1992b)

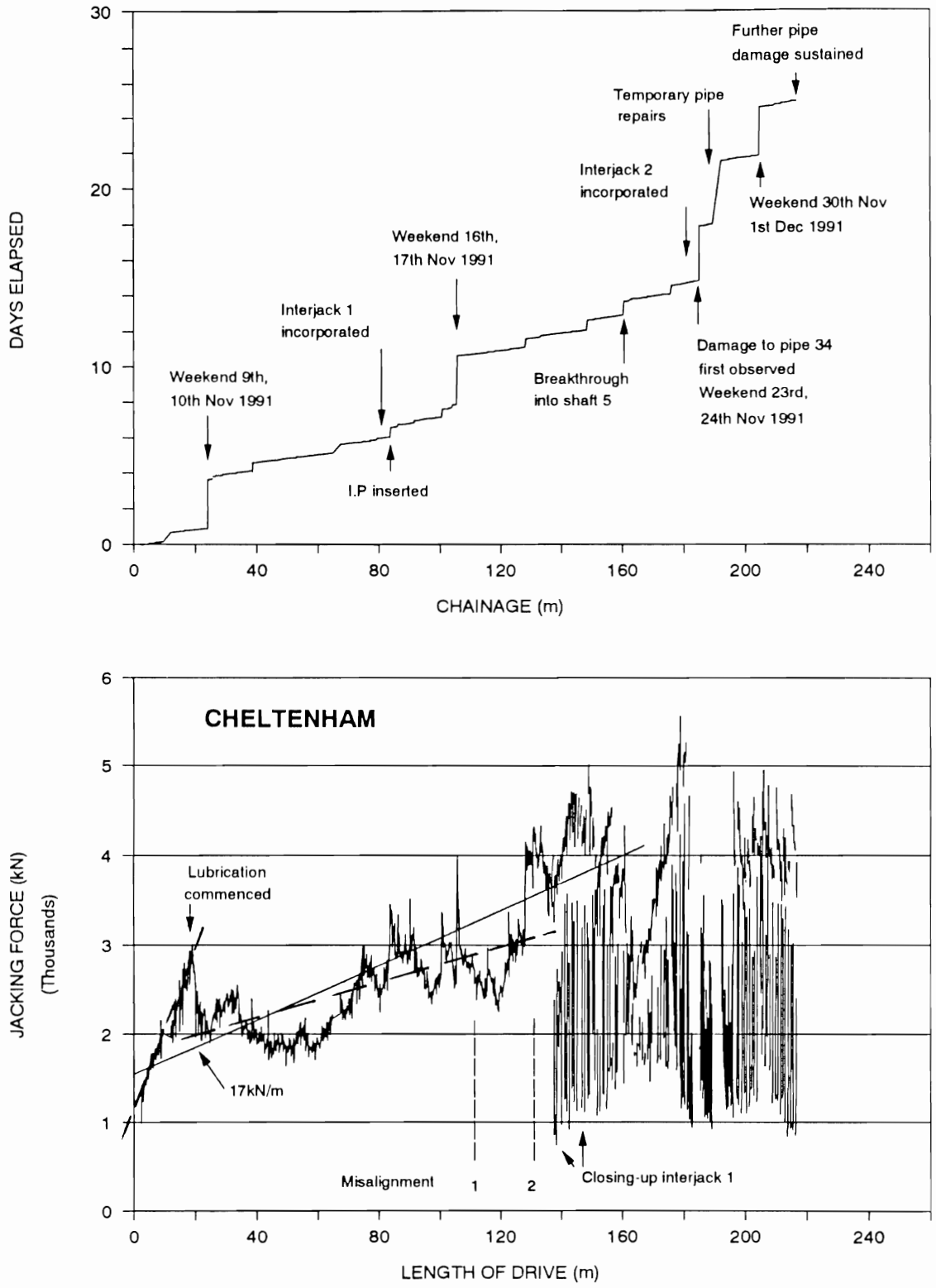

Figure 5.5 Jacking records for scheme 5 (Norris 1992b)

Cohesive with a stable bore
Haslem (1986)

$F = \alpha . s_u \, b$

where $\alpha . s_u$ is the "adhesion" between the pipe and clay.
b is the contact width.

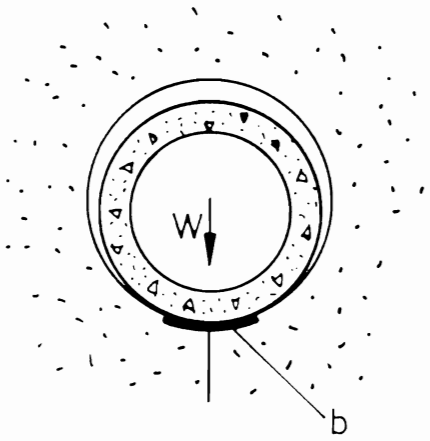

$b = 1.6(Pu*kd*Ce)^{1/2}$

where
Pu = contact force per unit length
$kd = D_1*D_2/(D_1-D_2)$
D_1 = internal diameter of the cavity
D_2 = external diameter of the pipe
$Ce = (1-n_1^2)/E_1+(1-n_2^2)/E_2$
E_1 = elastic modulus of the soil
E_2 = elastic modulus of the concrete pipe
n = Poisson's ratios as for E

Scheme	γ	h	E_1	E_2	n_1	n_2	P_u	D_1	D_2
	(kN/m^3)	(m)	(MPa)	(GPa)			(kN/m)	(m)	(m)
1	22	1.5	48	40	0.2	0.2	17.7	1.554	1.530
2	22	11	120	40	0.2	0.2	23.0	1.724	1.700
3	21	16av	96	40	0.2	0.2	35.3	2.304	2.280
4	18	7	144	40	0.2	0.2	24.2	1.804	1.780
5	19	6	144	40	0.2	0.2	-2.2*	1.450	1.430

For scheme 1, b = 0.30m and, from Figure 4.3c, $\alpha.s_u$ = 80kPa approximately.

Then $F = \alpha.s_u.b$ = 24kN/m, compared with a measured value of 29.8kN/m.

Figure 5.6 Model for ground loading in cohesive soil, after Haslem (1986)

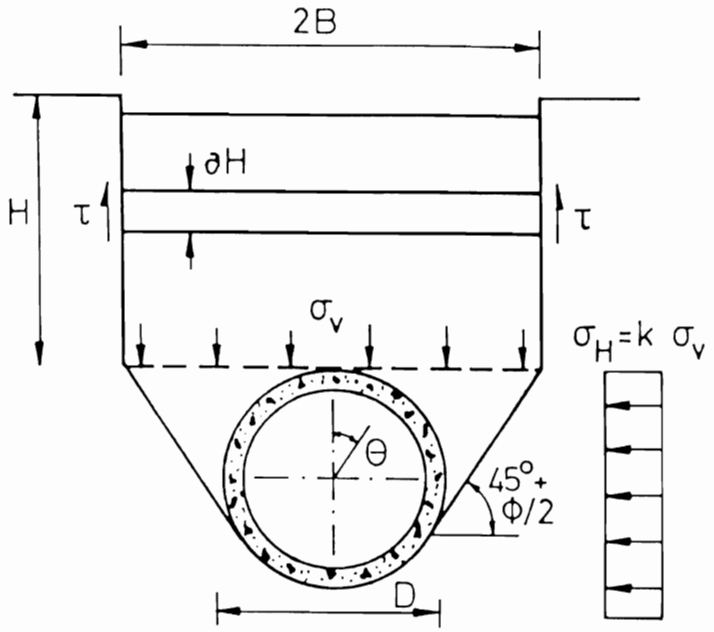

$$\sigma_v = \frac{\gamma . B}{k.\tan\phi}(1 - e^{k.\tan\phi . H/B})$$

$$\sigma_h = k(\sigma_v + 0.5\gamma . D)$$

The radial stress around the pipe is

$$\sigma_p = \frac{(\sigma_v + \sigma_h)}{2} + \frac{(\sigma_v - \sigma_h)}{2}\cos 2\theta$$

and the total frictional resistance is

$$F = \frac{\pi D}{2}(\sigma_v + \sigma_h).\tan\delta$$

where ϕ is the angle of internal friction of the soil, and
δ is the angle of friction between the pipe and the soil.

For scheme 5:-

ϕ = 32°, D = 1.45m, B = 1.23m, H = 4.675m, γ =19 kN/m^3

Then k = (1 - sin ϕ)/(1 + sin ϕ) = 0.307

and total jacking force F = 104kN/m

taking $\delta = 0.87\phi$

In addition, weight of pipe is 11.9kN/m, giving friction due to selfweight = 6.3 kN/m

Total calculated frictional resistance is 110kN/m, compared with measured resistance of approximately 2000kN over first 20m, or 100kN/m.

Figure 5.7 Model for ground loading in cohesionless soil, after Auld (1982), Terzaghi (1943).

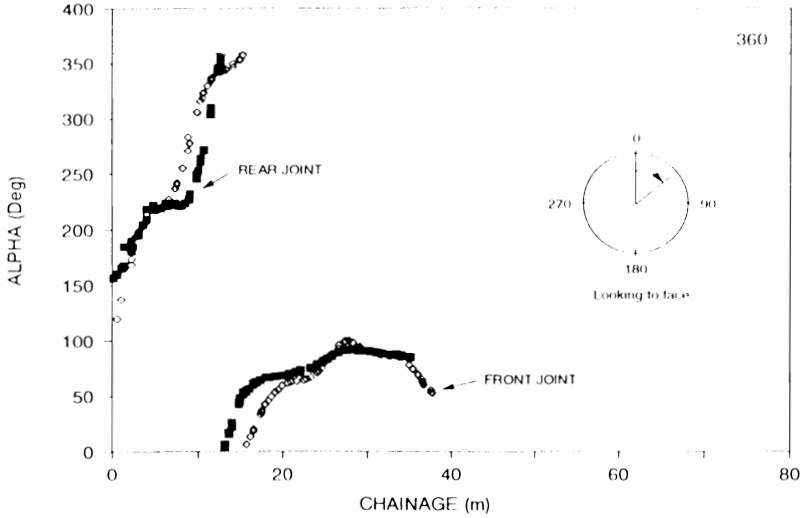

Comparison of the points of maximum compression in the front and rear joints at similar chainages throughout scheme 3.

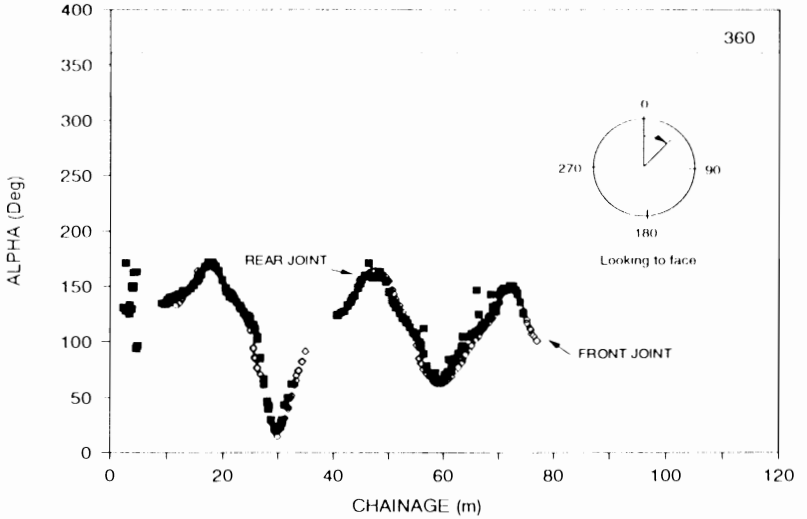

Comparison of the points of maximum compression in the front and rear joints at similar chainages throughout scheme 4.

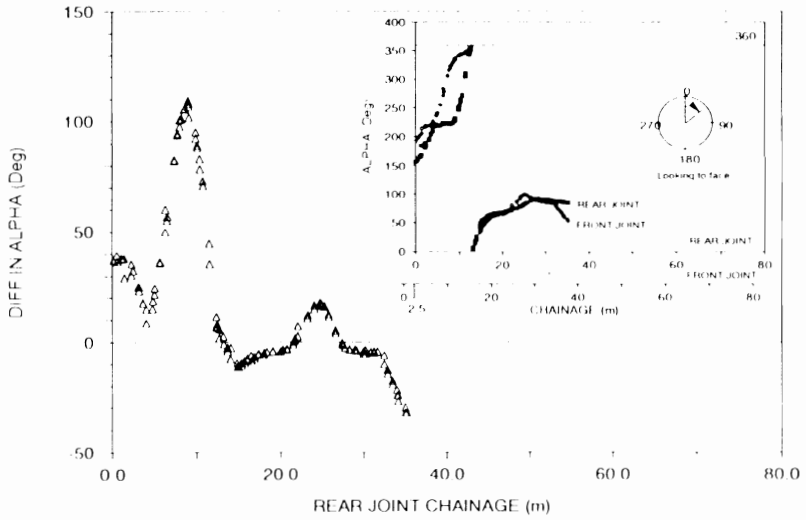

Figure 6.1 Angular difference between the front and rear points of maximum compression; scheme 3 (Norris 1992b)

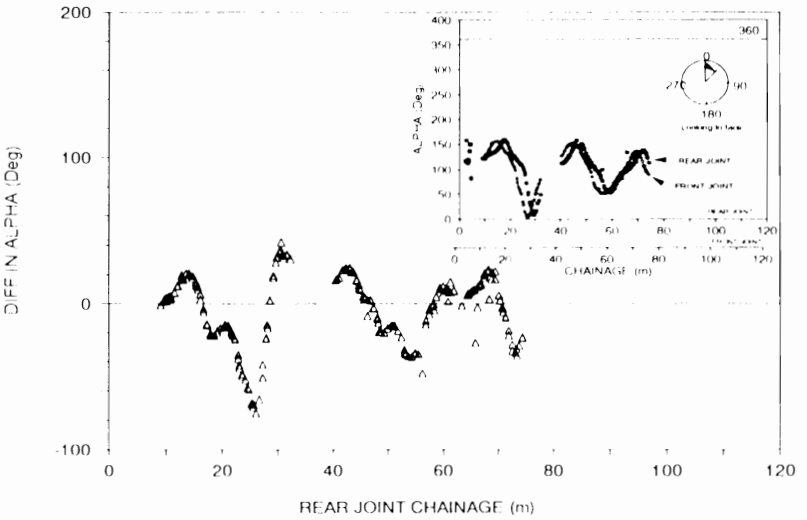

Figure 6.2 Angular difference between the front and rear points of maximum compression; scheme 4 (Norris 1992b)

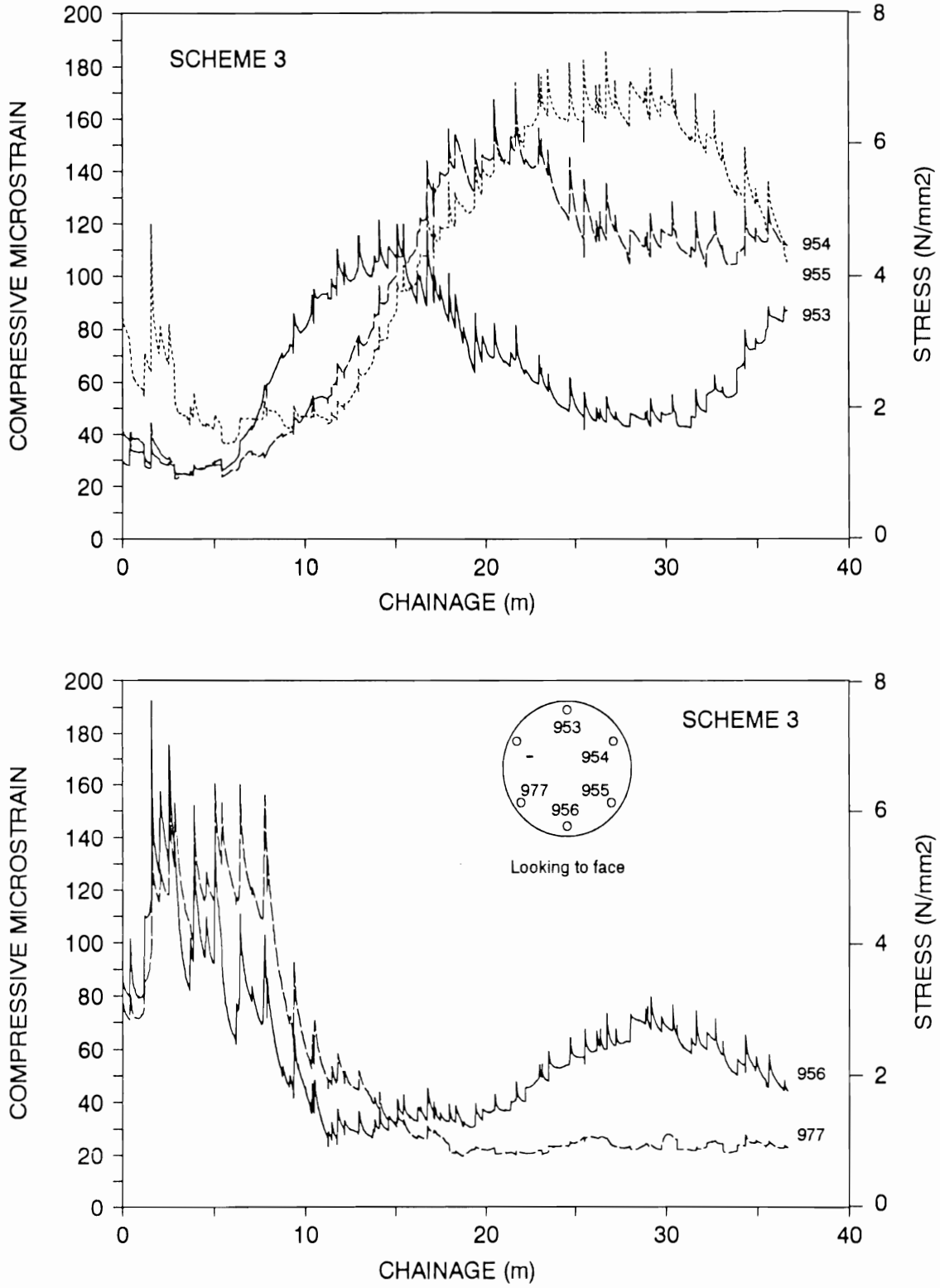

Figure 6.3 Average longitudinal pipe strains during jacking on scheme 3 (Norris 1992b)

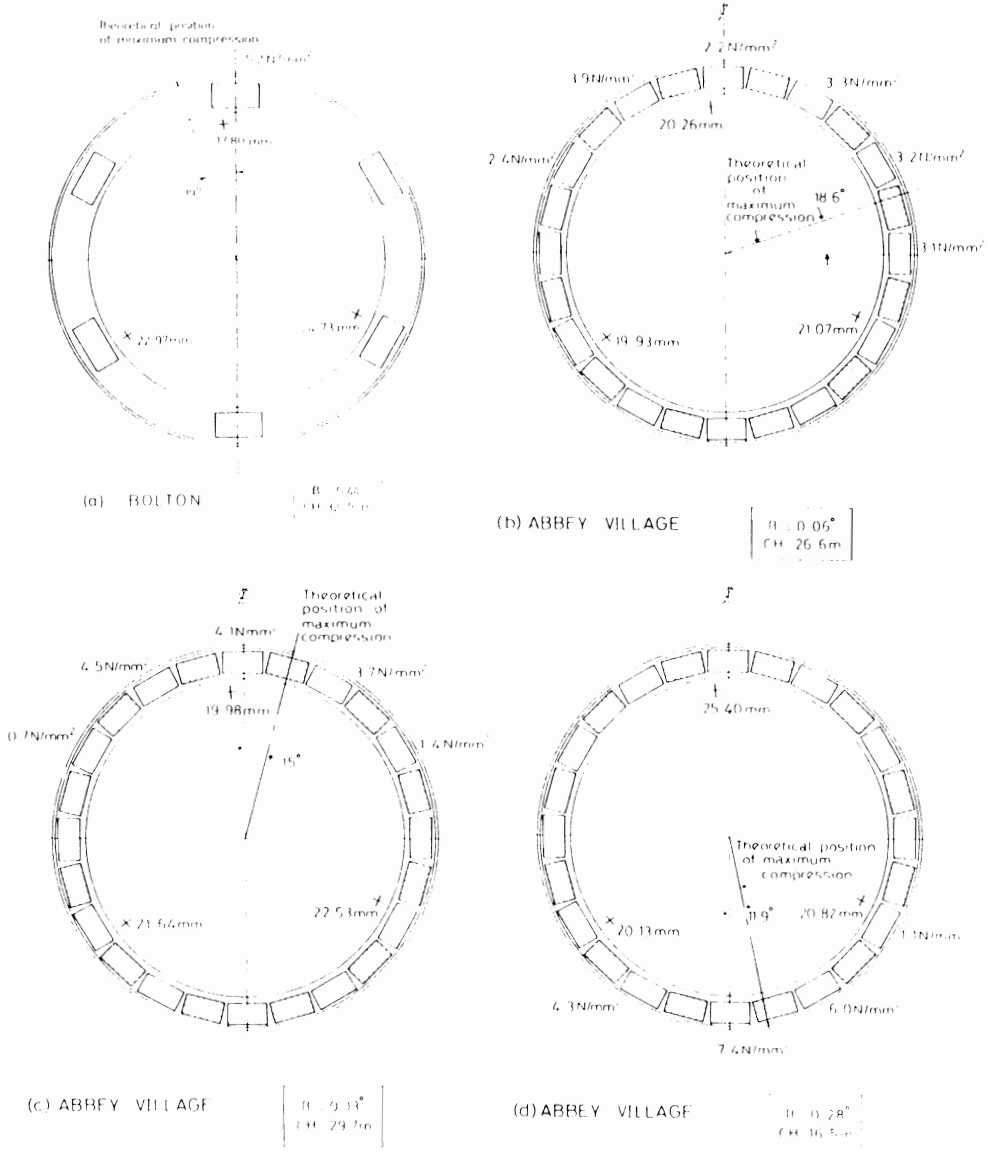

Figure 7.1 Relation between measured joint angle and pressure distribution; schemes 1 and 4 (Norris 1992b)

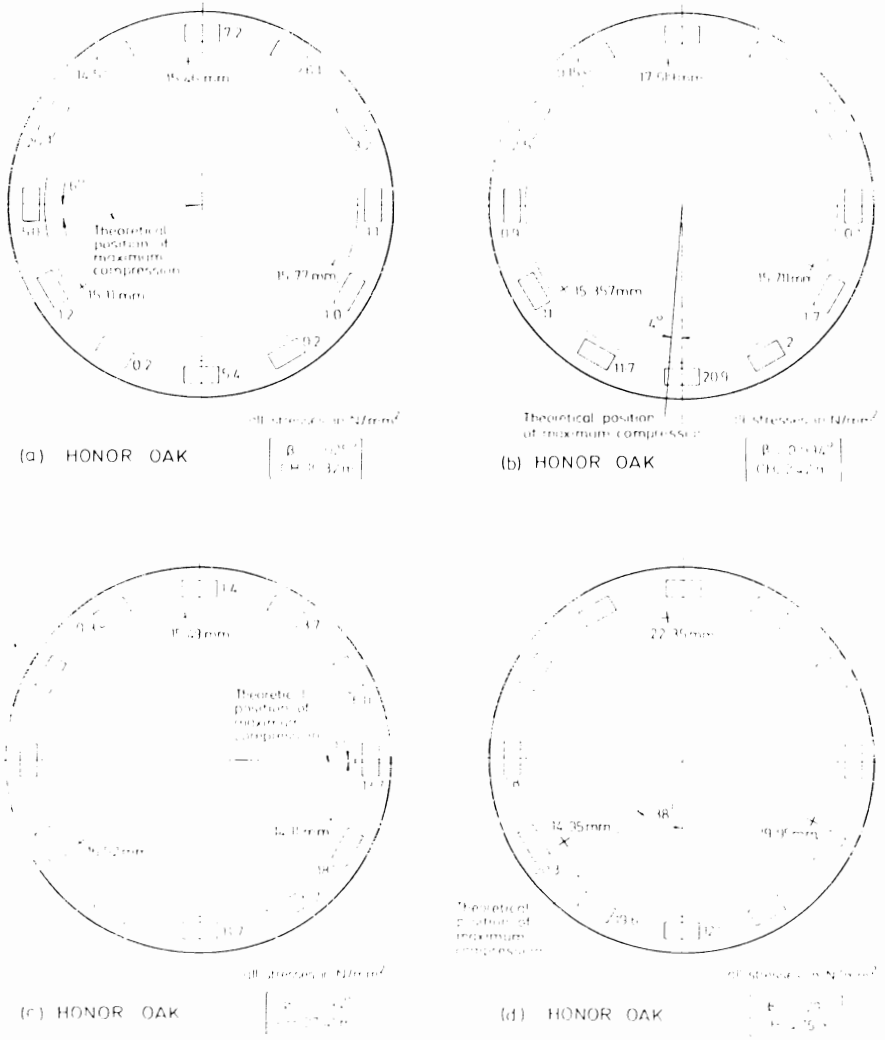

Figure 7.2 Relation between measured joint angle and pressure distribution; scheme 3 (Norris 1992b)

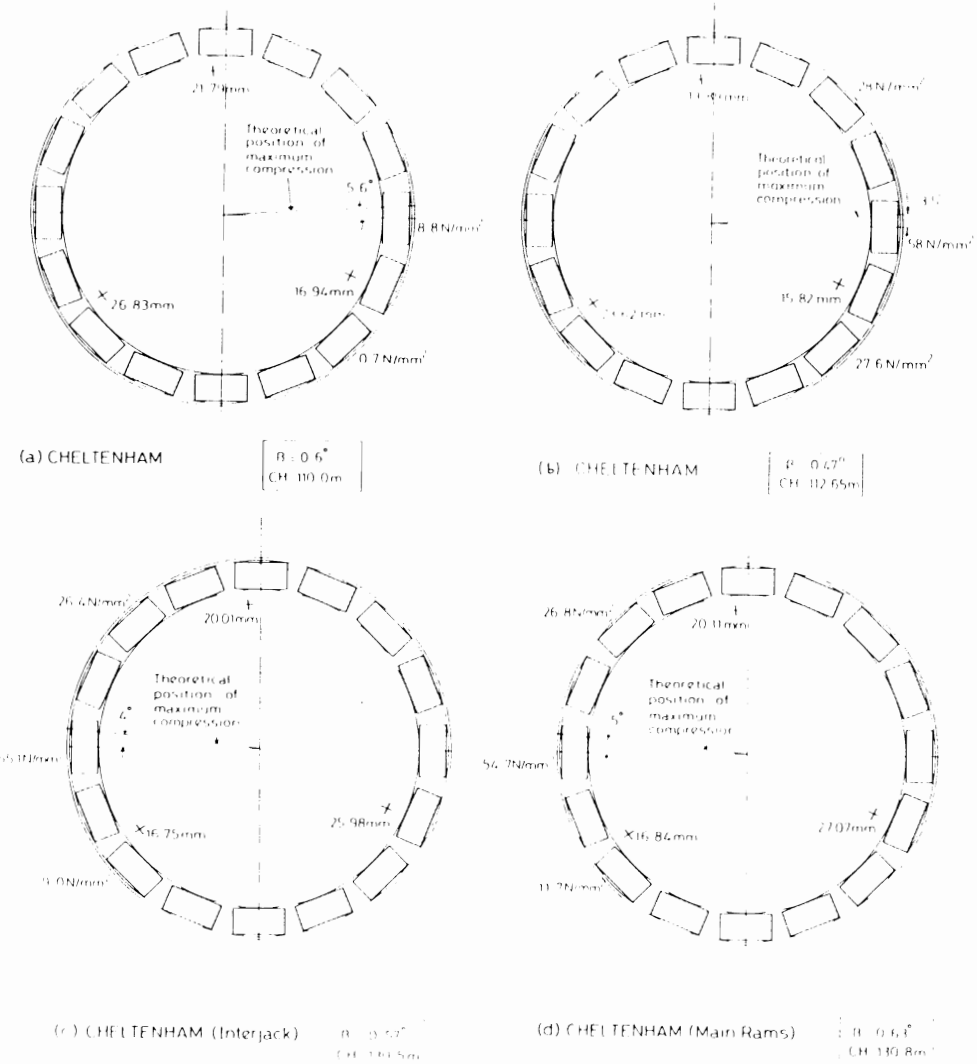

Figure 7.3 Relation between measured joint angle and pressure distribution; scheme 5 (Norris 1992b)

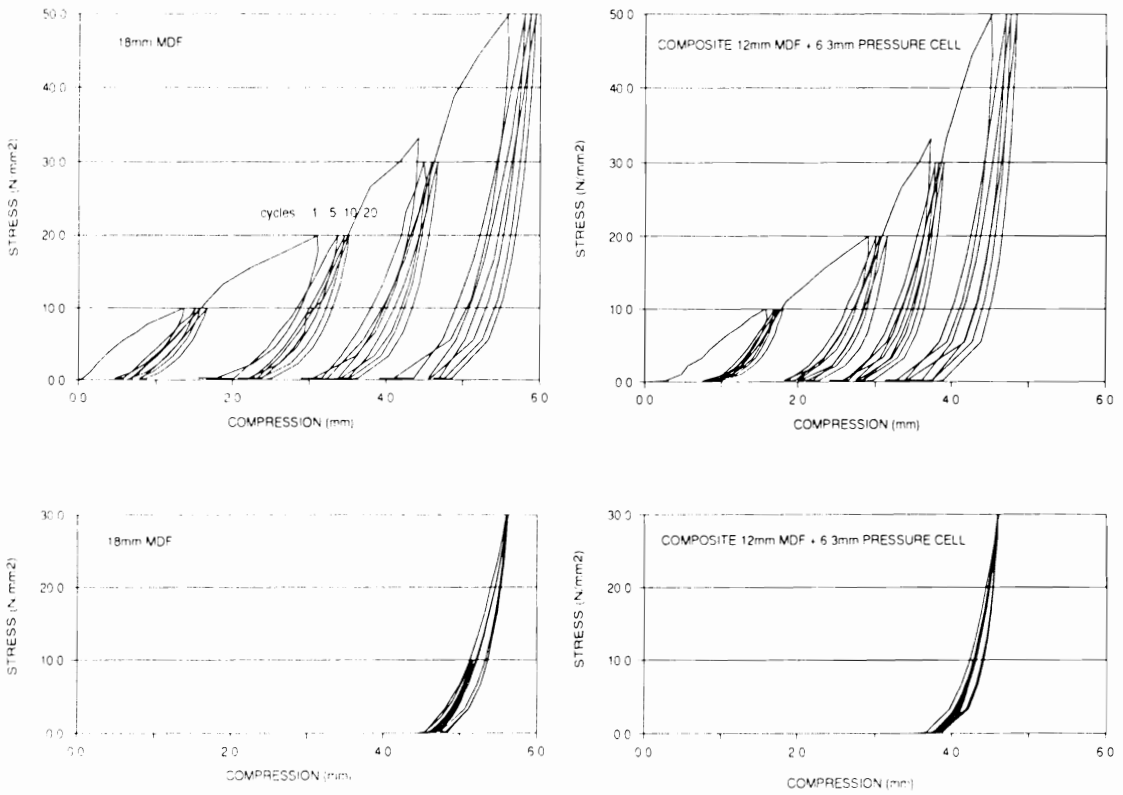

Figure 7.4 Uniaxial compression tests on joint packer material (Norris 1992b)

From the Australian Concrete Pipe association linear stress approach

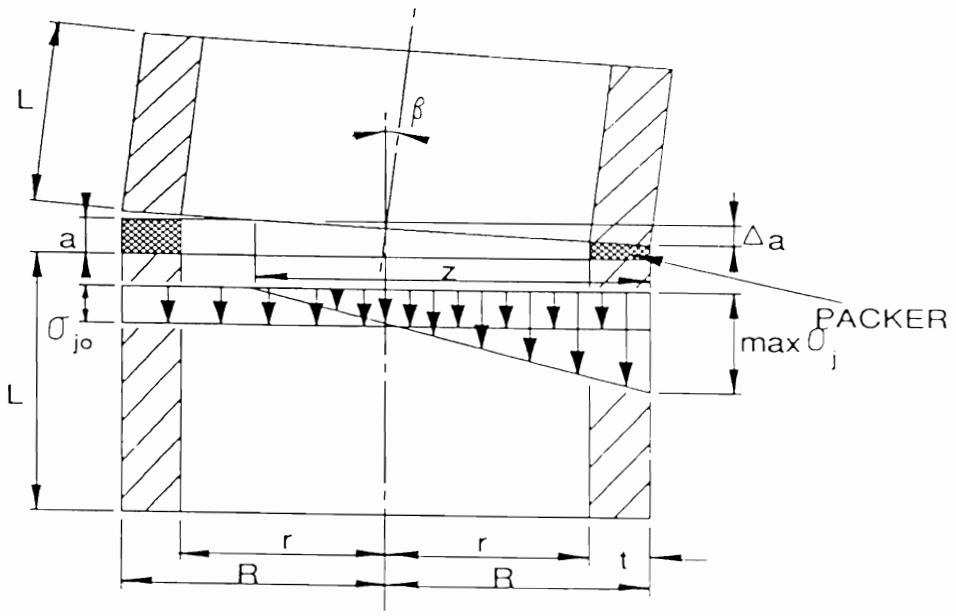

$$z = \frac{180}{\pi} \frac{a}{E_p} \frac{\max \sigma_j}{\beta}$$

Total force over hatched area for linear distribution of stress

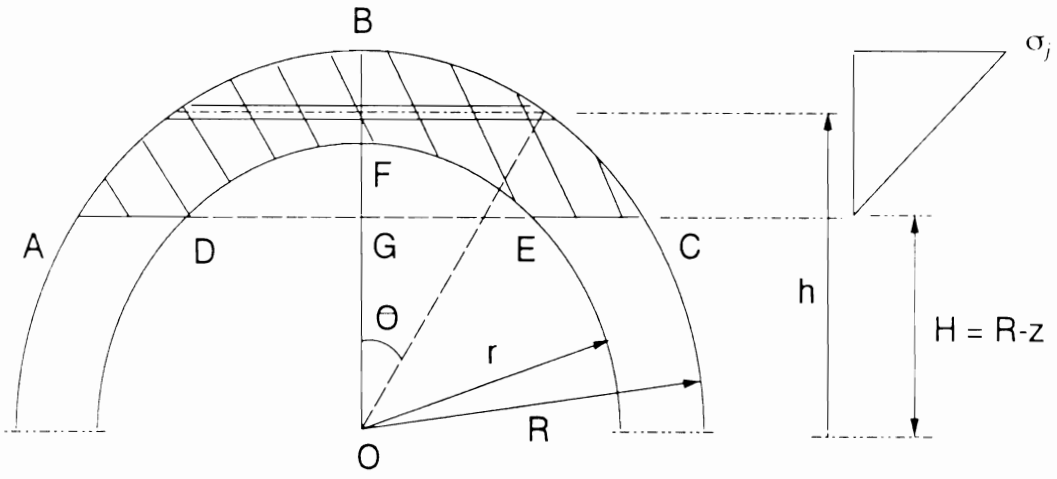

When H > r $F_{permissible}$ =

$$\frac{\sigma_j}{(R-H)} \left\{ 2/3[(R^2-H^2)^{3/2}] - H\left[R^2 \cos^{-1}\left(\frac{H}{R}\right) \right] + H^2 (R^2-H^2)^{1/2} \right\}$$

Figure 7.5 Jacking forces from linear joint stress model (Norris 1992b)

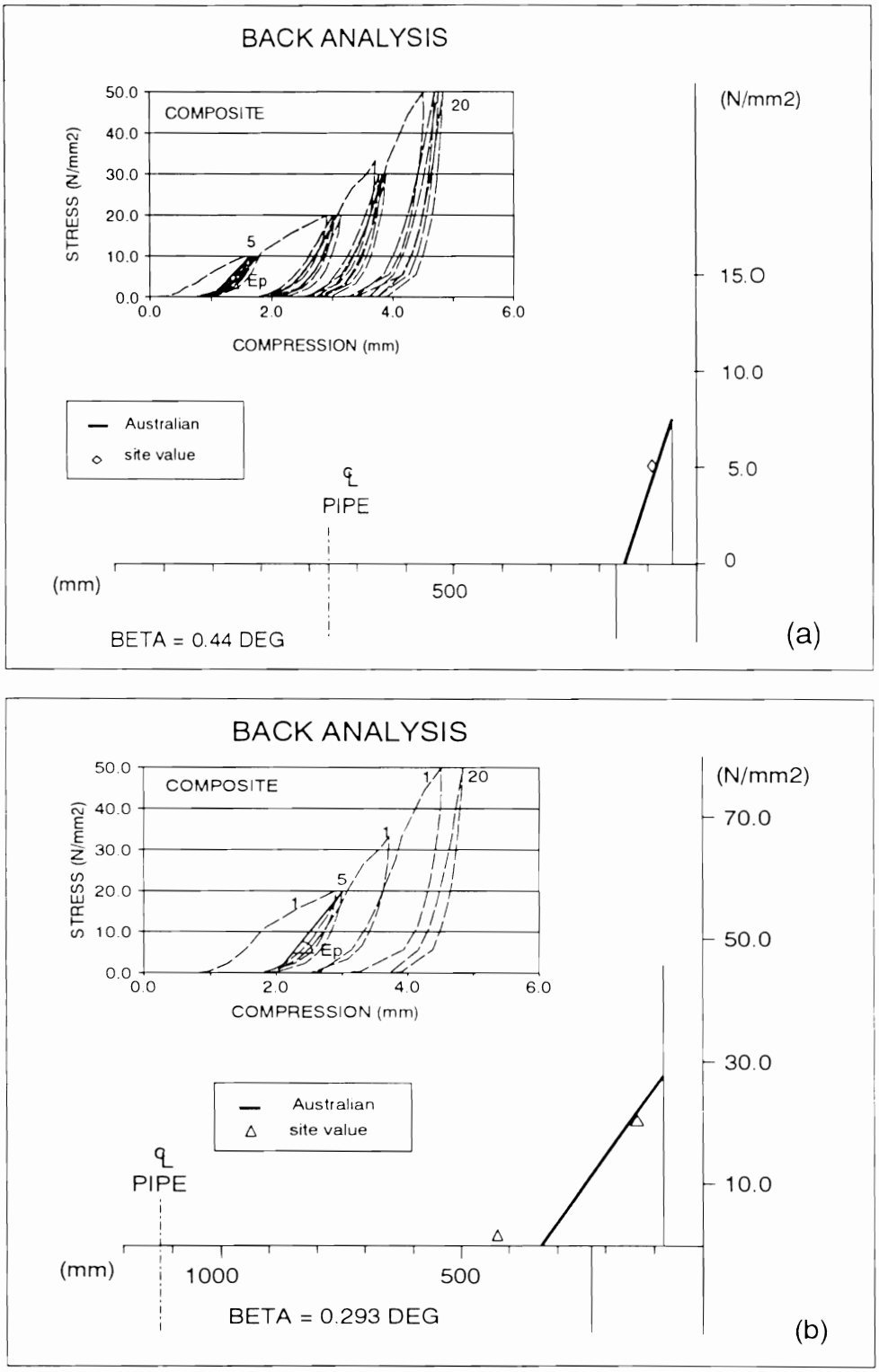

Figure 7.6 Comparison of measured joint stress distribution to predicted using a linear stress model based on the Australian Concrete Pipe Association method. (a) scheme 1 rear joint subject to a β value of 0.44°, and (b) scheme 3 rear joint subject to a β value of 0.29°.

(Norris 1992b)

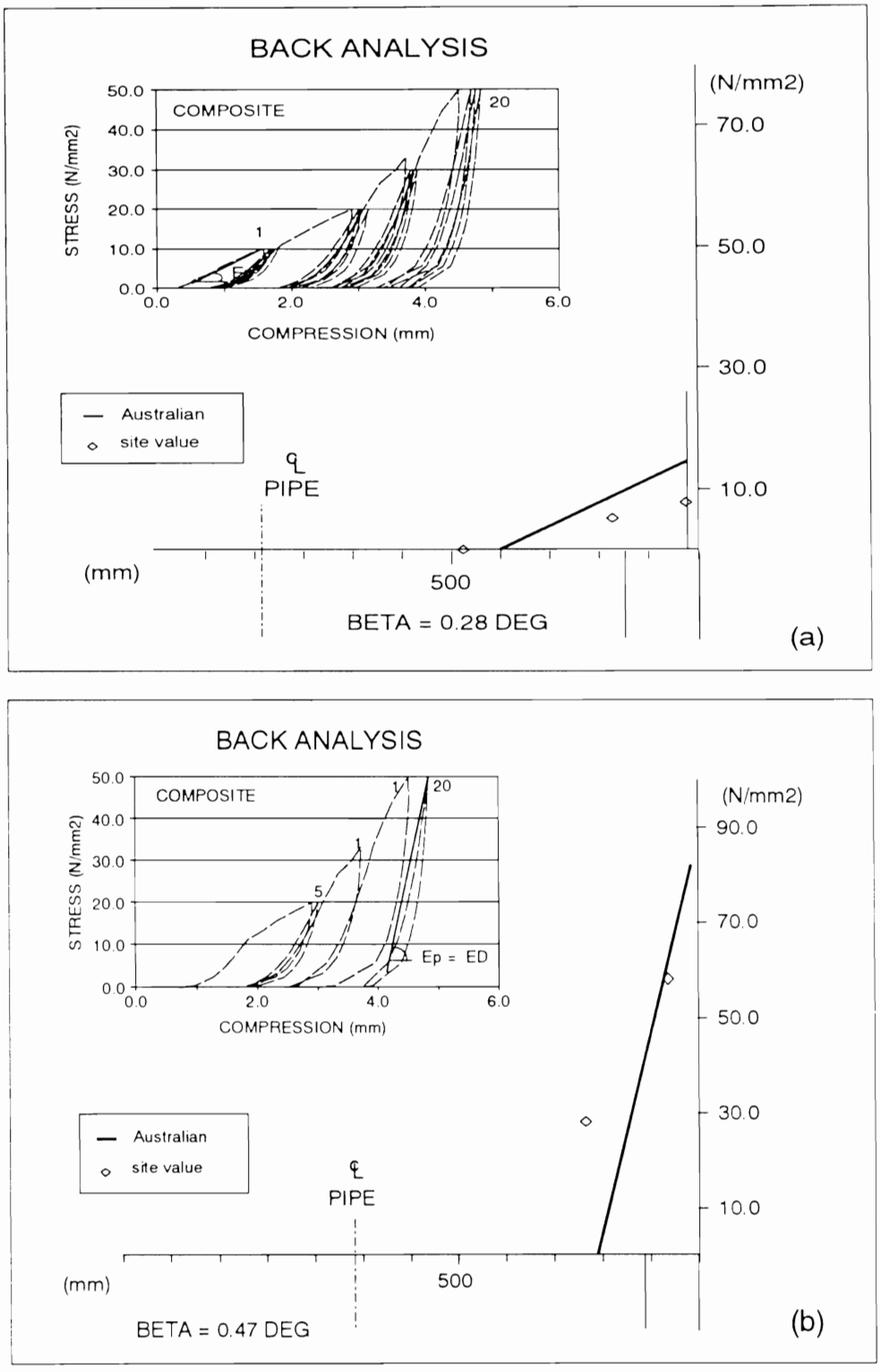

Figure 7.7 Comparison of measured joint stress distribution to predicted using a linear stress model based on the Australian Concrete Pipe Association method. (a) scheme 4 rear joint subject to a β value of 0.28°, and (b) scheme 5 rear joint subject to a β value of 0.47° and pipe damage.

(Norris 1992b)

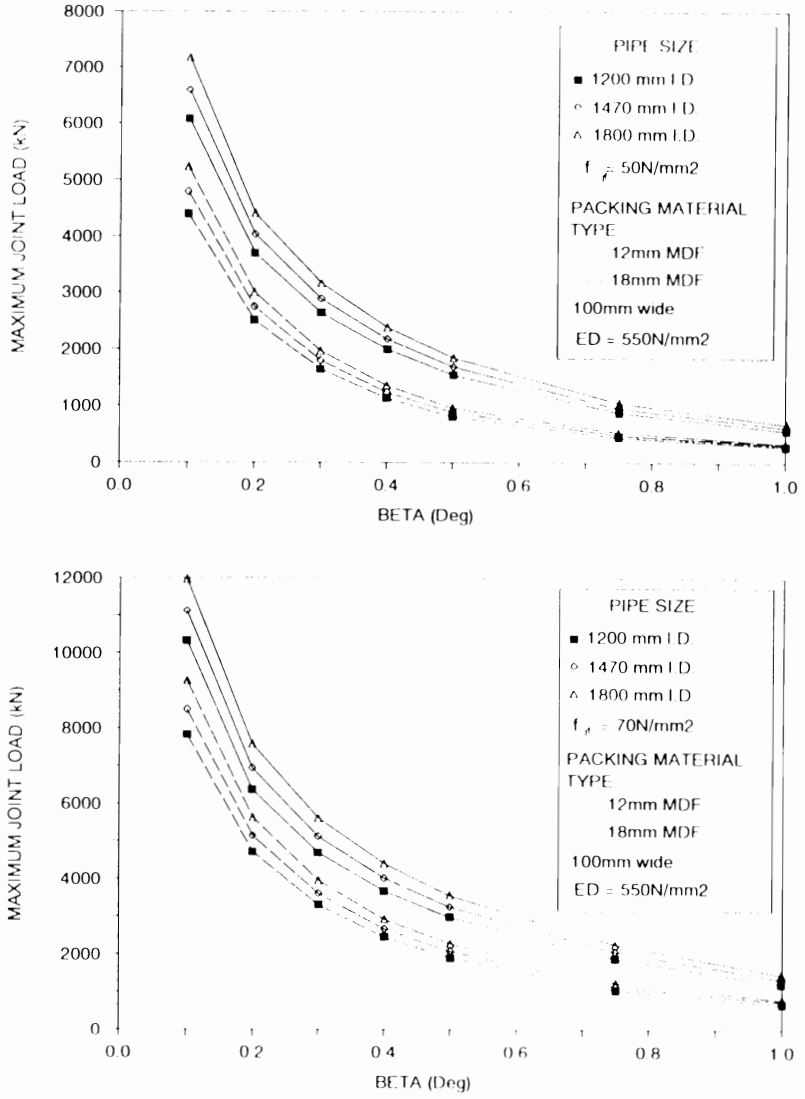

Figure 7.8 Permissible pipe end loading at various angular misalignments; 100mm wide medium density fibreboard (Norris 1992b)

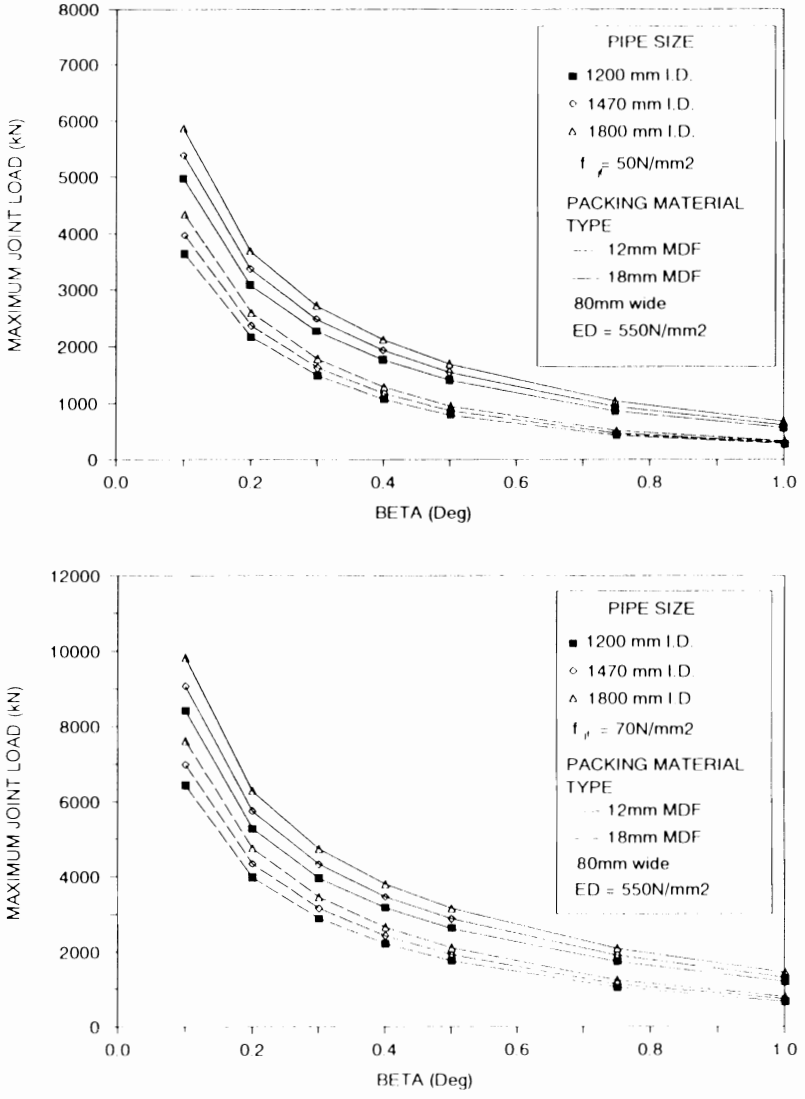

Figure 7.9 Permissible pipe end loading at various angular misalignments; 80mm wide medium density fibreboard (Norris 1992b)

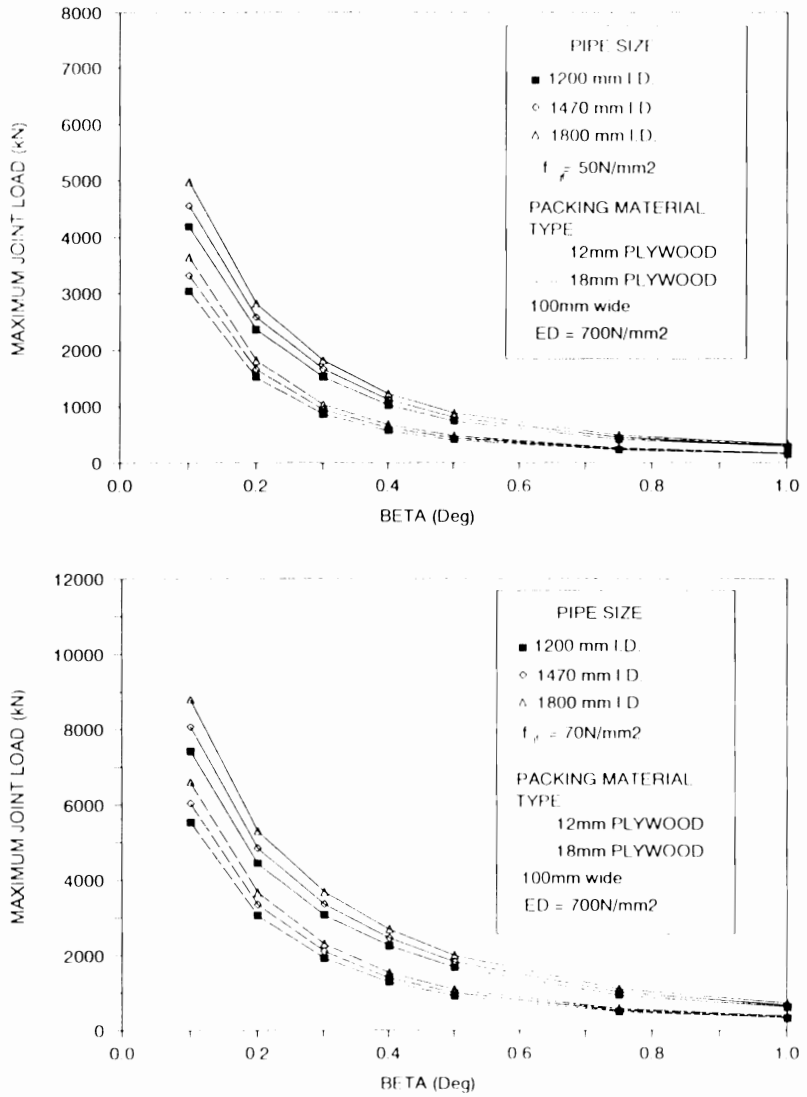

Figure 7.10 Permissible pipe end loading at various angular misalignments; 100mm wide exterior grade plywood (Norris 1992b)

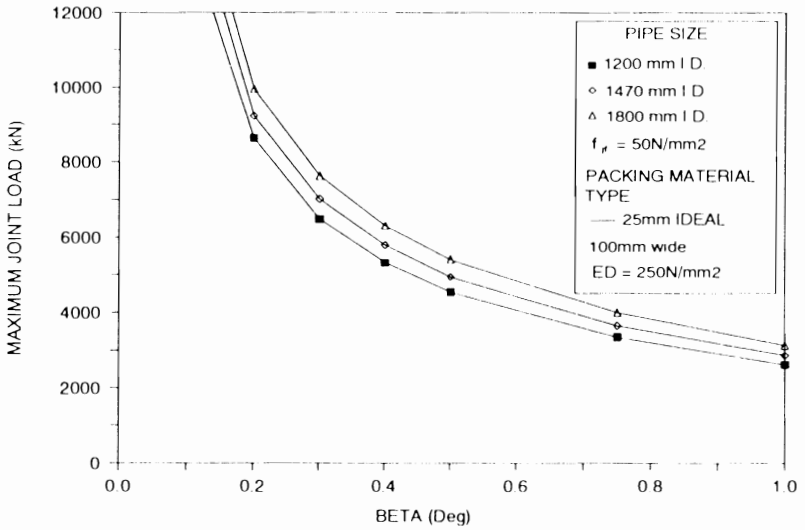

Figure 7.11 Permissible pipe end loading at various angular misalignments; 100mm wide idealised packing material (Norris 1992b)

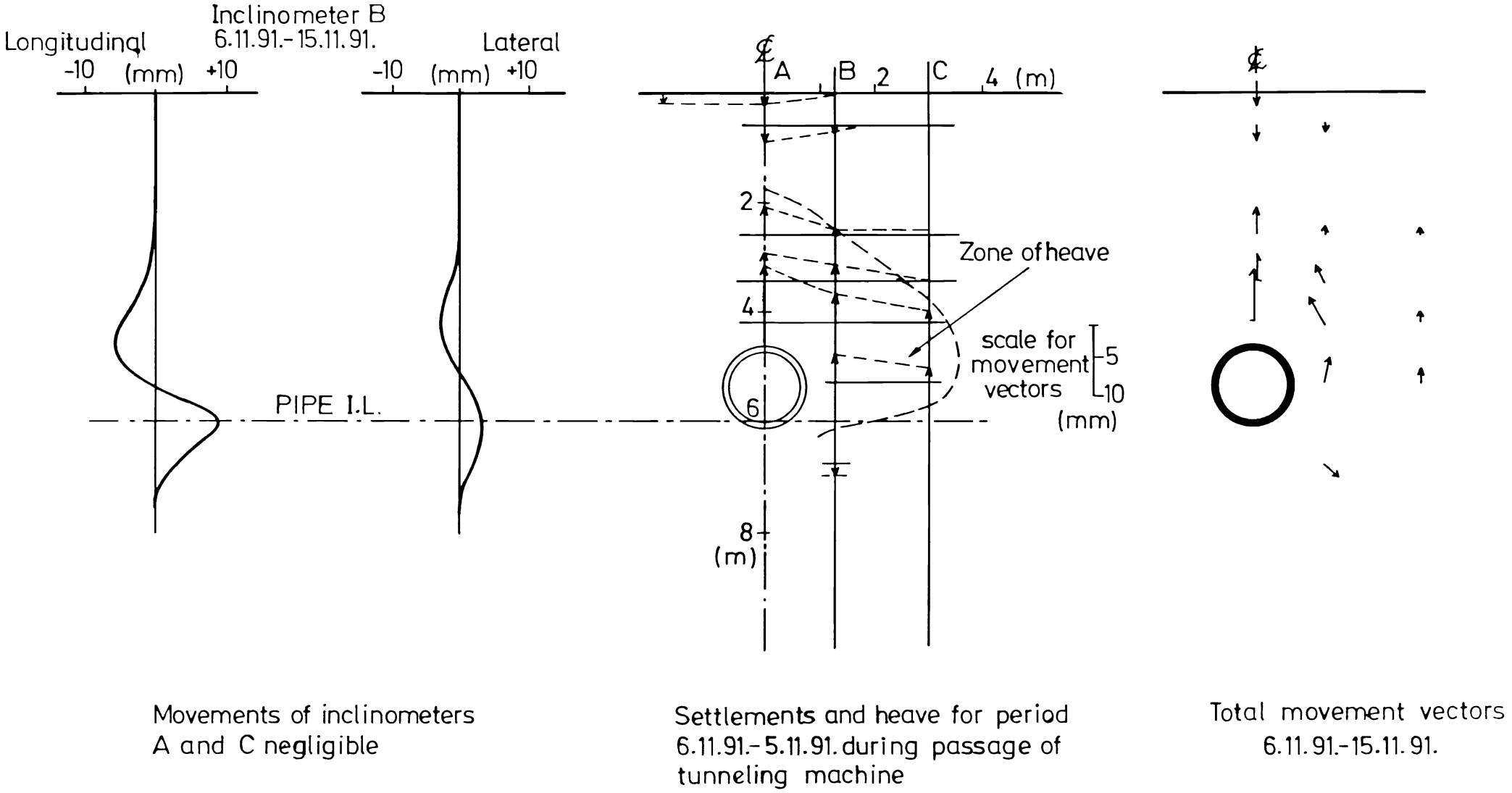

Movements of inclinometers
A and C negligible

Settlements and heave for period
6.11.91.-5.11.91. during passage of
tunneling machine

Total movement vectors
6.11.91.-15.11.91.

Figure 8.1 Measured ground movements due to passage of tunnelling machine; scheme 5

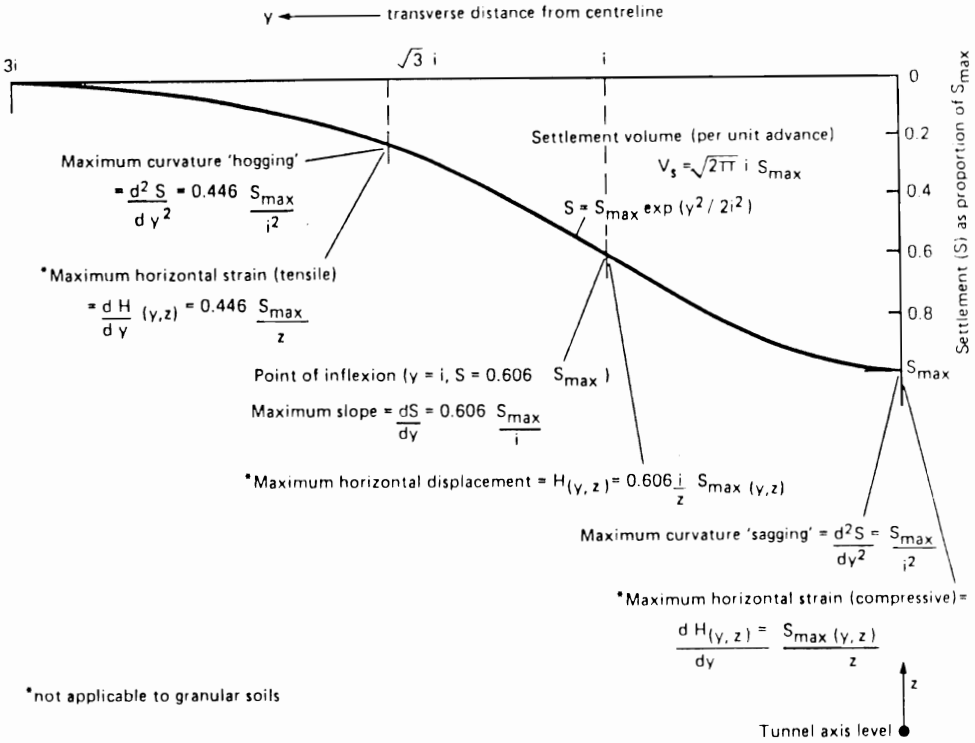

Settlement semi-profile with error function form

From O'Reilly and New (1982)

Surface settlement s is given by

$$s = s_{max} \cdot e^{-y^2/2i^2} = \frac{V_s}{\sqrt{2\pi} \cdot i} \cdot e^{-y^2/2i^2}$$

where V_s = volume loss/unit length.

For scheme 5 instrumented section
depth to tunnel axis z = 5.4m
from plot b) i = 1.4m

Volume of overbreak

$$V_s = \frac{\pi}{4}(1.45^2 - 1.43^2) = 0.045 m^3/m$$

giving s_{max} = 12.8 mm

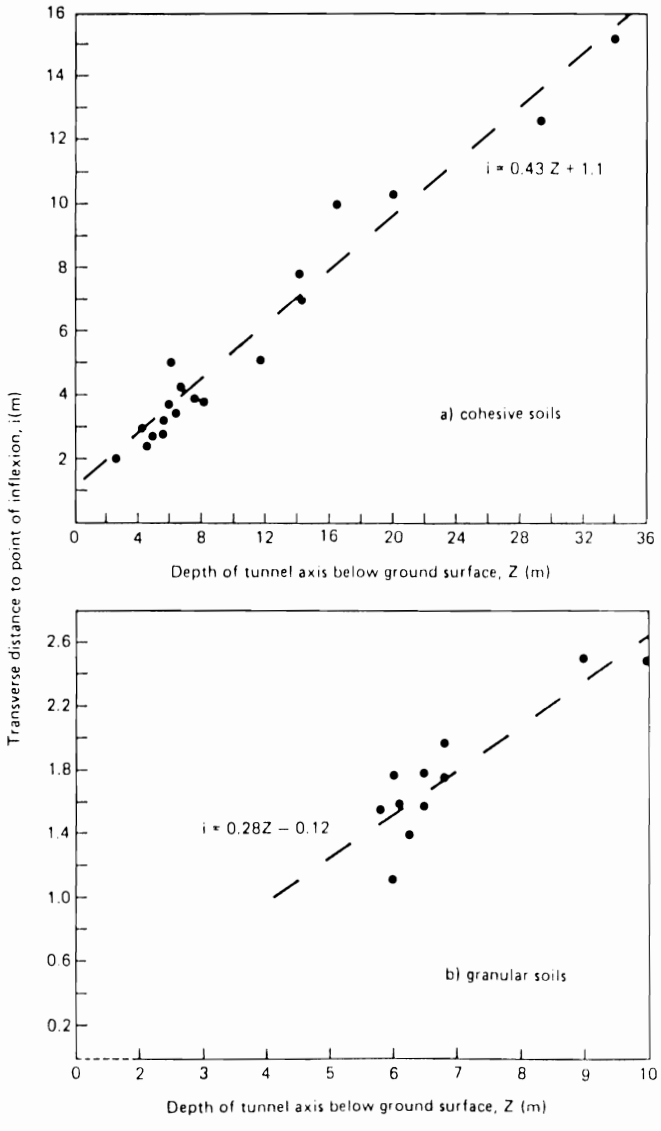

Variation of trough width parameter, i, with tunnel depth

Figure 8.2 Calculation of long-term settlements

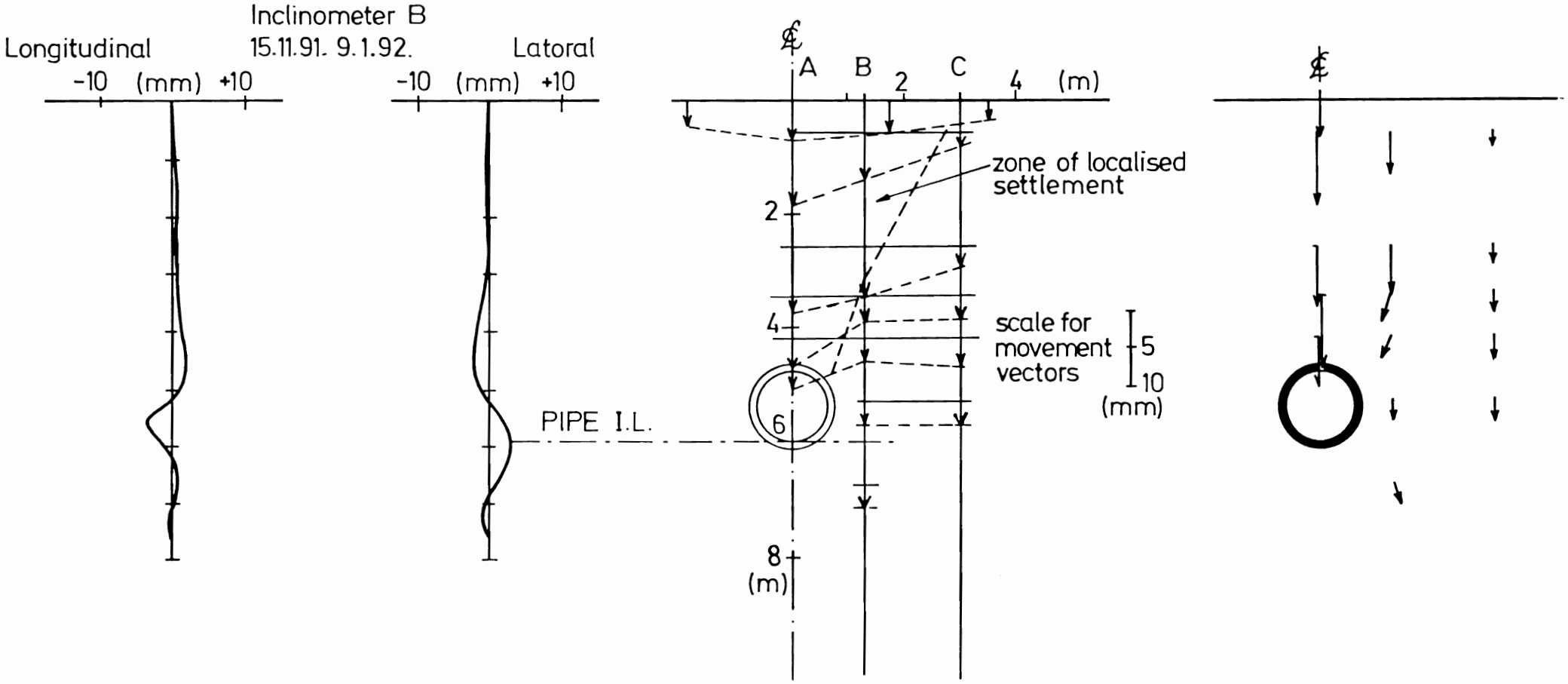

Movements of inclinometers
A and C negligible

Settlements for period 15.11.92–9.1.92. following passage of tunneling shield.

Total movement vectors
15.11.91.–9.1.92.

Figure 8.3 Measured long-term settlements; scheme 5

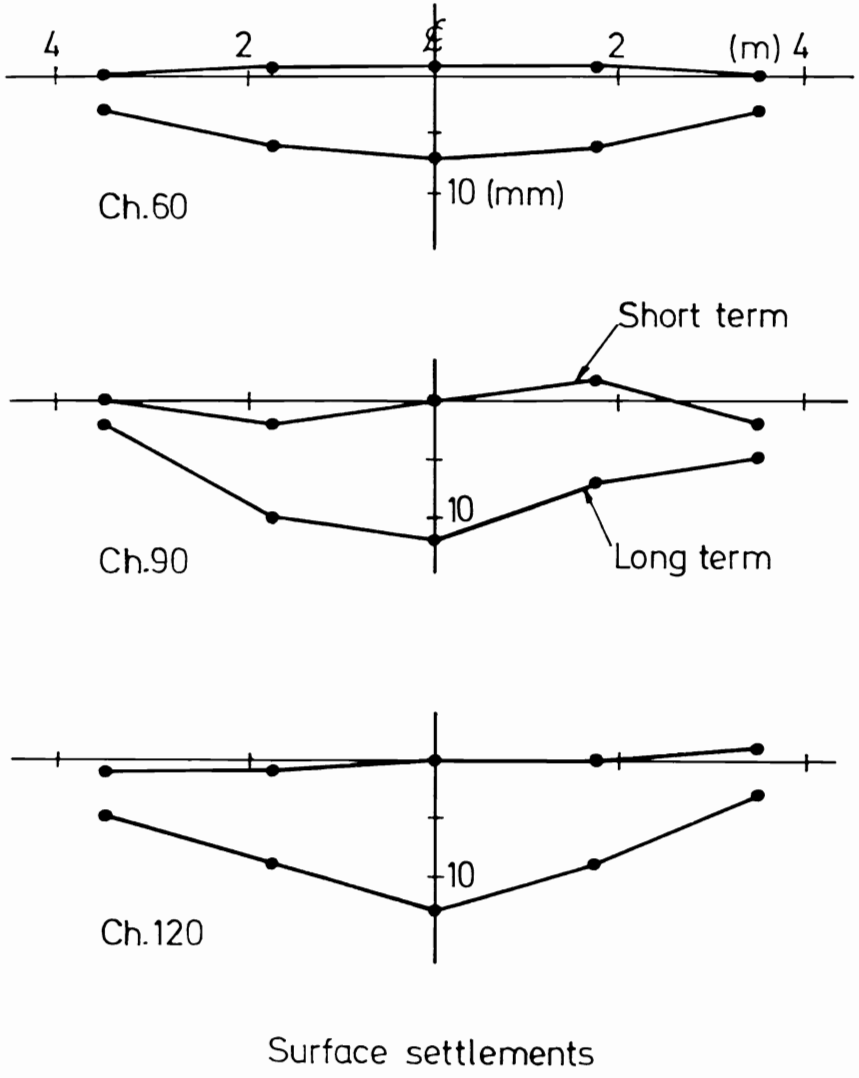

Figure 8.4 Measured surface settlements at three cross-sections; scheme 5

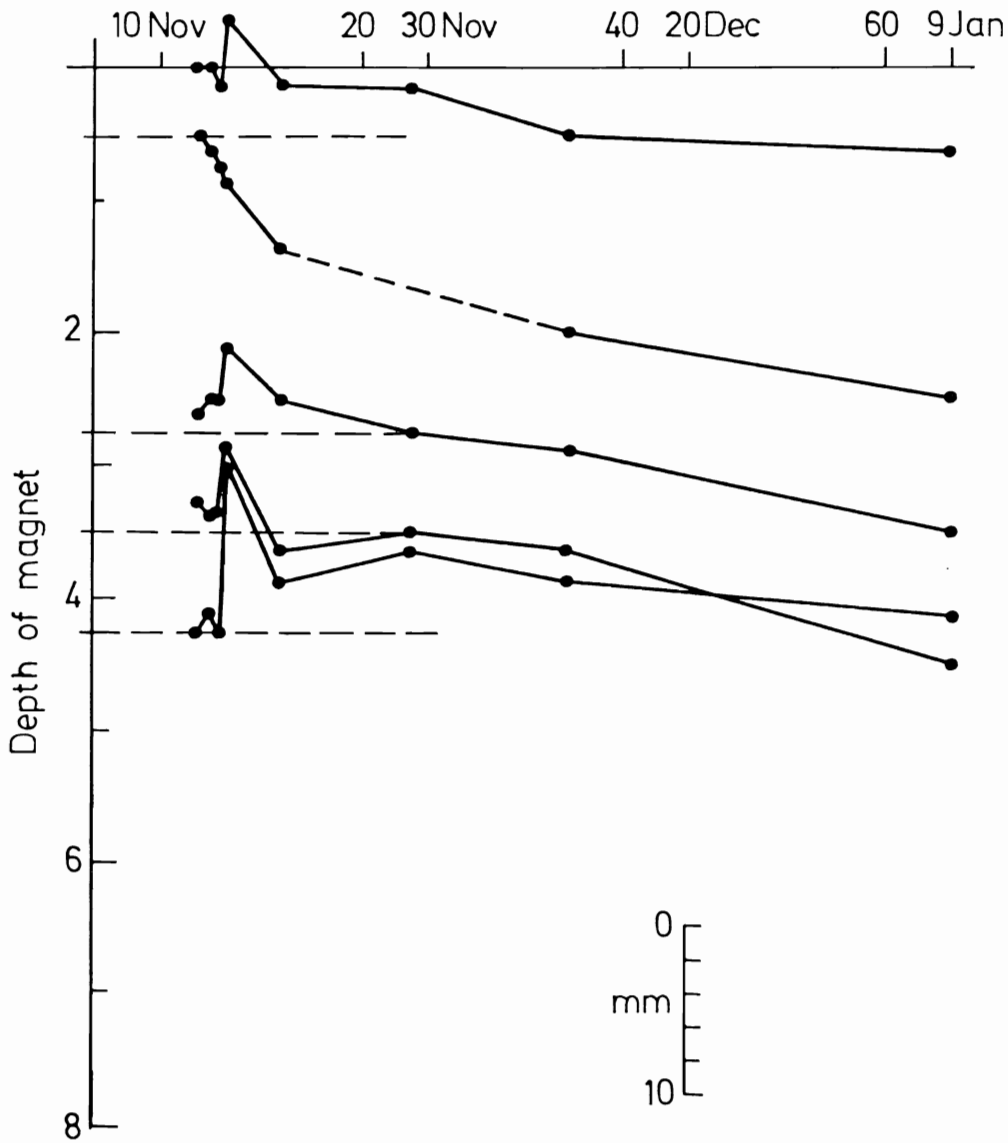

Figure 8.5 Variations with time of ground movements on tunnel centreline; scheme 5